Mar Geophys Res (2015) 36:1–34
DOI 10.1007/s11001-014-9230-z

ORIGINAL RESEARCH PAPER

Tectonic evolution of the northern shelf of the Marmara Sea (Turkey): interpretation of seismic and bathymetric data

Huseyin Tur · Nihan Hoskan · Gulten Aktas

Received: 20 January 2014 / Accepted: 4 July 2014 / Published online: 19 July 2014

Abstract This study is based on the geological interpretation of 250 km^2 of multibeam bathymetric data coupled with 300 km of seismic profiles recorded on the northern shelf of the Marmara Sea offshore Büyükçekmece and Küçükçekmece Lagoons. The sea bottom morphology has a highly chaotic structure at the exit of the Büyükçekmece and Küçükçekmece lagoons. This chaotic surface structure is controlled by a basin-ridge system lying in the NE–SW direction at the exit of the Büyükçekmece Lagoon and by a relatively deep entrance observed at the exit of the Küçükçekmece Lagoon. In addition, the linear submarine slope parallel to the shoreline between the Istanbul Strait and the Küçükçekmece Lagoon is an important morphological structure of this area. The Istanbul Strait's canyon on the northern shelf of the Marmara Sea and the elevated submarine plain west of this canyon are other important morphological structures observed at the sea bottom. The geologic interpretation of seismic profiles has allowed us to distinguish two seismo-stratigraphic units. The lower one is separated from the overlying units by a seismic sequence having a seismic facies from chaotic to parallel and the top represented by a high amplitude seismic reflector. Since these units get close to the sea bottom rising landwards, they are inferred to be the seaward continuation of the Oligocene–Upper Miocene units widely exposed on land. The upper unit, overlying the acoustic basement, whose parallel internal reflections onlap and downlap on the top of the acoustic basement, is interpreted as a Quaternary basin fill. Two groups of faults have been identified on seismic profiles and identified based on their characteristics in the study area. The first group consists of dip-slip faults trending NNE–SSW. These faults border the western slope of the Bosporus and the NNE–SSW trending basins offshore of the Büyükçekmece Lagoon. The second group of faults consists of NW–SE oriented strike-slip faults. These faults have created the linearities in the same direction at the sea bottom. As the result of comparison of these NW–SE-faults to the North Anatolian Fault Zone (NAFZ), this group of faults is likely to have a relation with the NAFZ. Therefore, it is considered that the mentioned faults may be reactivated in the region due to the stress created by the NAFZ.

Keywords Northern Marmara Sea shelf · North Anatolian Fault (NAF) · Shallow seismic · Multibeam bathmetry · Lagoons

H. Tur (✉) · N. Hoskan
Geophysics Department, Engineering Faculty, Istanbul University, Avcılar, Istanbul, Turkey
e-mail: tur@istanbul.edu.tr

G. Aktas
Engineering and Nature Sciences Faculty, Gumushane University, Baglarbası, Gumushane, Turkey

Introduction

The Anatolian Block is located on the Alpine–Himalayan Mountain Range developed by the African-Arabian (Gondwanaland) and Asian-European (Laurasia) continents which collided as the result of the subduction of the ocean (Tethys). The Anatolian Block evolved in the above mentioned collisional zone, taking its current shape (Sengör and Yilmaz 1981).

Two large fault zones formed as the result of the westward movement of Anatolia. The first one, i.e. the North Anatolian Fault Zone (NAFZ), easily shows itself today with many morphological elements lying somewhat parallel with the Black Sea coast along the north of the

Anatolian Block (Fig. 1). It provides significant conveniences for geologists working in this area to identify this fault and its effects (e.g. Sengör 1979; Sengör et al. 2005; Barka and Kadinsky-Cade 1988). The second one is the left-lateral strike-slip East Anatolian Fault (Fig. 1). The NAFZ divides into two branches near Bolu and enters the Marmara Sea throughout the Gulfs of İzmit and Gemlik right at the west of this area (Fig. 1). These faults, which can be well observed on land, are much more difficult and expensive to observe and identify at sea because of the requirement of high technology. This has resulted in model-based interpretations for the behavior of the NAFZ in the Marmara Sea rather than data-based research for many years.

The last stage of this tectonic evolution is still going on today, as the Anatolian block is moving westward throughout the NAFZ and East Anatolian Fault Zone, resulting from the collision of the African-Arabian and Eurasian plates across Eastern Anatolia (Fig. 1; Ketin 1948; Sengör 1979, 1980). The westward migration of the Anatolian block is quantified as 20 mm/year between these two fault zones and has been clearly identified through GPS measurements (McClusky et al. 2000; Fig. 2.)

Several geological studies have dealt with the discussion of the NAFZ in the Marmara Sea and related stratigraphic aspects. Barka and Kadinsky-Cade (1988) have discussed the strike-slip fault geometry in Turkey and its influence on earthquake activity. Alavi et al. (1989) have investigated the Late Quaternary sedimentation in the İstanbul Strait through high resolution seismic profiles. Demirbag et al. (1999) have discussed the last sea level changes in the Black Sea evidenced by the studies on seismic data. High resolution shallow seismic data collected from the south-western shelf of the Black Sea indicate five different seismo-stratigraphic units. Okay et al. (2000) have studied the active faults and the evolving strike-slip basins in the Marmara Sea through multichannel seismic. Imren et al. (2001) have discussed the North-Anatolian Fault within the Marmara Sea based on the interpretation of multichannel seismic and multibeam bathymetric data. 2,200 km of multichannel seismic reflection profiles that have become recently available in the Sea of Marmara have been analyzed. Le Pichon et al. (2001) have discussed the active Marmara fault based on bathymetric and seismic reflection data. Armijo et al. (2002) have discussed the asymmetric slip partitioning in the Sea of Marmara pull-apart basin as a clue to propagation processes of the North Anatolian Fault. High-resolution geophysical data on the submarine fault system that forms a smaller pull-apart beneath the Northern Sea of Marmara, between two well-known strike-slip faults on land (İzmit and Ganos faults) have been collected and discussed. Gazioglu et al. (2002) have discussed the morphological features of the Marmara Sea from multibeam data. Oktay et al. (2002) have examined the effects of the NAFZ on the latest connection between the Black Sea and the Marmara Sea. The development of the Istanbul Strait is also one of the principal results of the tectonics which led to the evolution of the NAFZ in the Marmara Region 3.7 Ma ago. Yaltirak (2002) has studied the tectonic evolution of the Marmara Sea and its surroundings. Ergintav et al. (2011) have discussed the structural framework onshore and offshore Avcilar (Istanbul, Turkey) under the influence of the North Anatolian Fault. To investigate the onshore/offshore structural framework of the northern shelf of the Sea of Marmara, a multidisciplinary study was carried out, including multichannel and single-channel seismic reflection profiles, multibeam bathymetry, sidescan sonar images on offshore as well as land studies for S-wave velocity estimation by passive and active array measurements and monitoring of block deformations by Global Positioning System (GPS). Akarvardar et al. (2009) monitored the Avcılar district by satellite radar interferometry between 1992 and 1999 for evaluating deformation in and around Avcılar. Algan et al. (2011) determined Holocene coastal change in the ancient harbor of Yenikapı–İstanbul. Dogan et al. (2013) determined the displacement field of the landslides by using GPS observations, measured in a regional network between 2007 and 2009. Yildiz and Karaman (2013) developed a probabilistic post-earthquake ignition model by considering real sources and applied this model in the Küçükçekmece District of İstanbul, Turkey.

The results of all the aforementioned studies have given rise to the need to carry out seismic and bathymetric studies in the north-eastern shelf of the Marmara Sea, whose young tectonic activity is not adequately known, in order to fill the data gap in this area and test the assertions summarized above. This study aimed to collect high resolution geophysical data to fill this lack of data, in particular for the area between Istanbul and the NAFZ. For this purpose, the Marmara Sea northern shelf remaining between the exit of the Istanbul Strait and the Gulf of Büyükçekmece was chosen and high resolution seismic and bathymetric data collected by the Turkish Navy, Department of Navigation, Hydrography and Oceanography (TN-DNHO) were examined.

One main aim of the paper is to test the results of previous studies on the submarine geomorphology, stratigraphy and tectonics of the Northern Marmara Sea through the multibeam and seismic data. Digital land topographic data and bathymetric data have been merged and on onshore-offshore Digital Elevation Model (DEM) of the study area has been constructed. Another aim is the identification of the faults on seismic profiles between the Gulf of Tuzla and the Istanbul Strait on the bathymetric maps and to establish their continuation towards the Bosphorus, more than to reveal if these faults are related with the structural elements

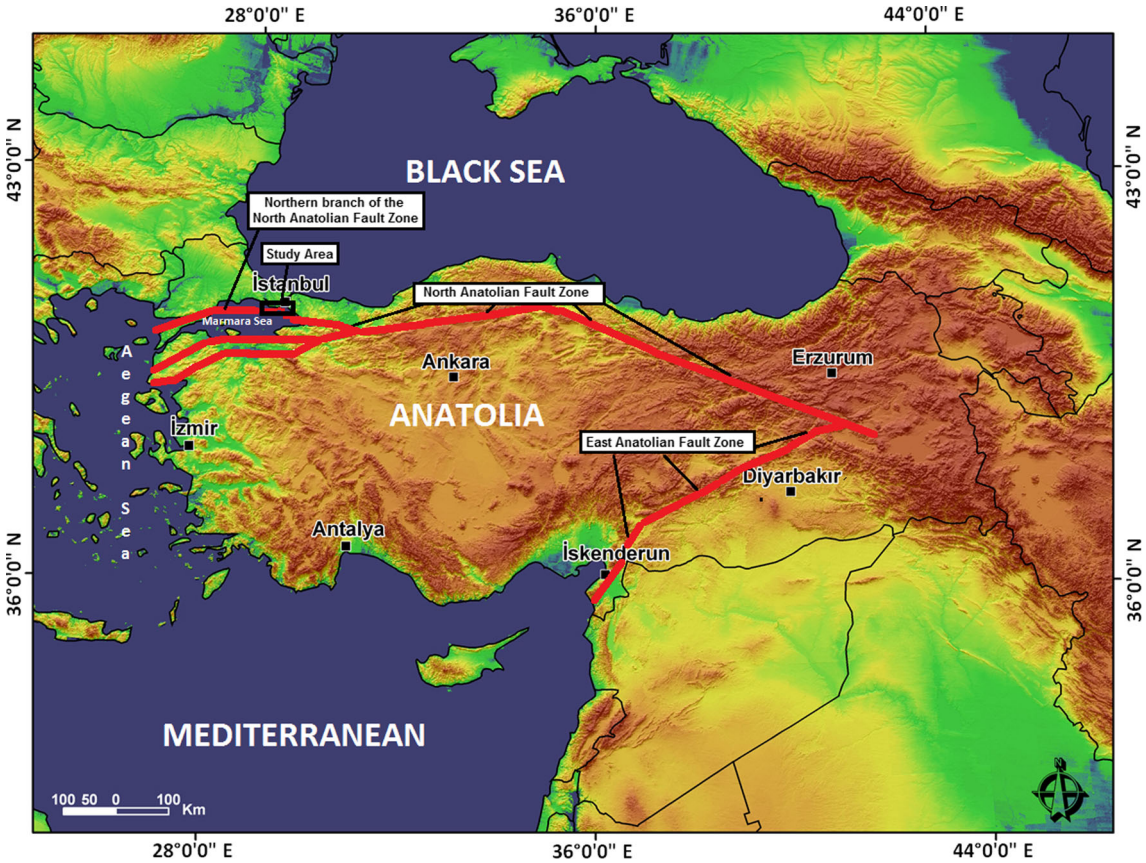

Fig. 1 Major fault zones in Anatolia

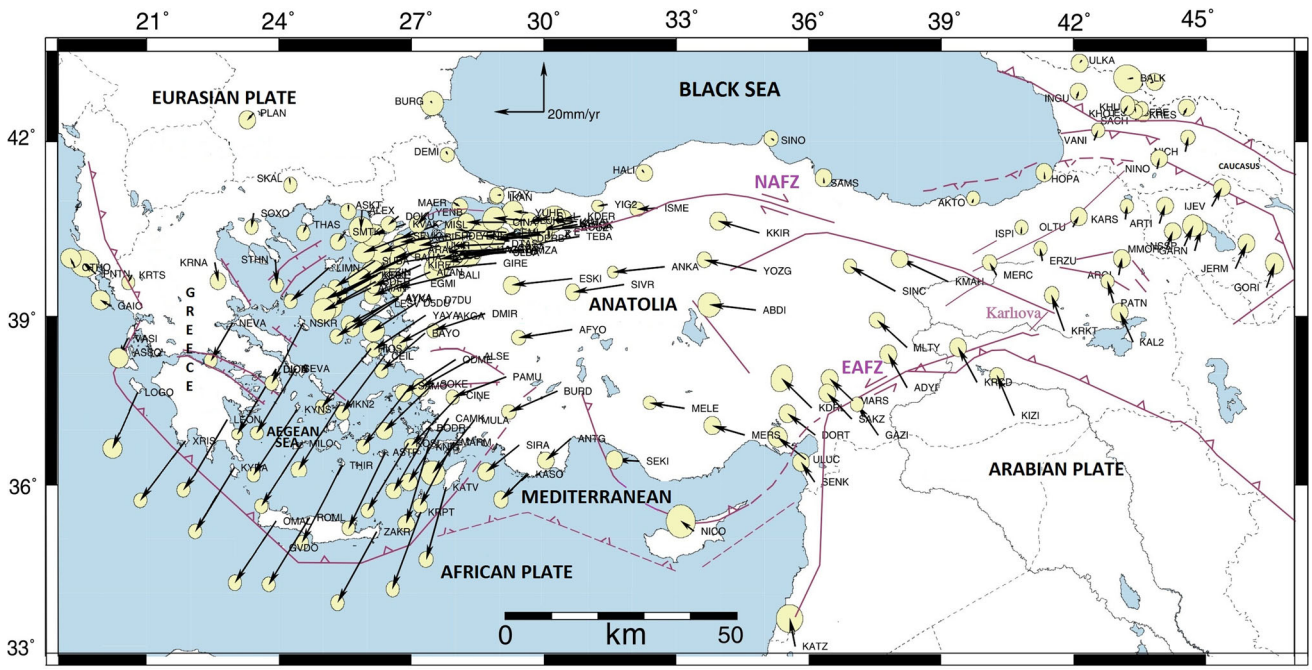

Fig. 2 Current movement vector of the Anatolia as the result of the GPS surveys conducted (McClusky et al. 2000)

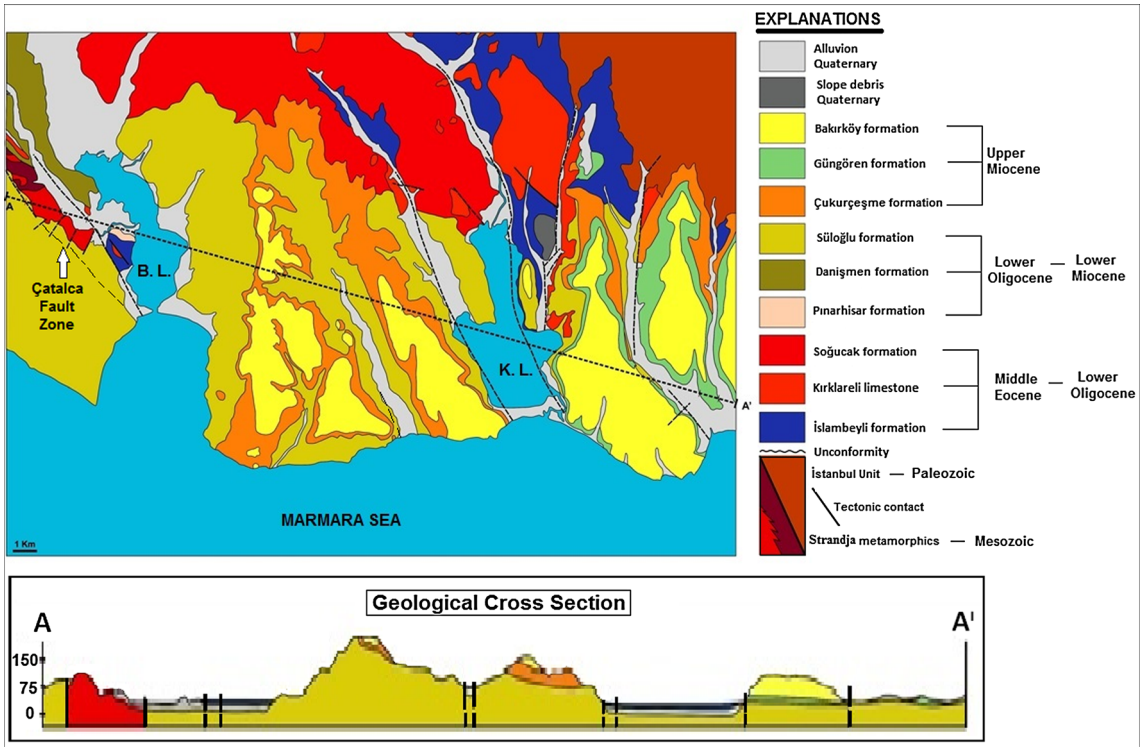

Fig. 3 Simplified geological map of the study area and surroundings (Tur et al. 2013)

already known offshore and onshore. Palaeotopographic maps of the seismic horizon representing the top of the acoustic basement identified on seismic section and interpreted as Oligo-Miocene terranes widely cropping out onshore in the adjacent sectors and basin fill thickness map of Quaternary deposits overlying the acoustic basement of the Northern Marmara Sea shelf have also been constructed.

Geological setting

The study area is located on the boundary between Istanbul Unit (Palaeozoic) and Strandja Massif (Palaeozoic–Mesozoic), and both are overlain by Eocene and younger sediments of Thrace basin (e.g. Okay et al. 2001). The Strandja Massif is composed of granitoids, phyllite and schist, which basset in the Çatalca Fault Zone, essentially a horst bounded by dipping faults (Fig. 3). The metamorphism age is Late Jurassic–Early Cretaceous (Okay et al. 2001, Sunal et al. 2006). The Istanbul Unit is consisted of turbiditic sandstone-shale sequence. This carboniferous sandstone-shale sequences basset at the northeast Küçükçekmece Lagoon (Fig. 3). Middle–Upper Eocene limestone units overlain on the Çatalca metamorphics in the west and on the Carboniferous flysch in the east for transgression; and the West Black Sea Fault (WBSF) (Fig. 4), a major dextral strike-slip fault zone, is covered by them (Okay et al. 1994). The Eocene limestones pass up into a clastic series of Upper Eocene–Oligocene separated by a major unconformity from the overlying Upper Miocene fluviatile to lacustrine deposits, portrayed by marn, limestone, shale and siltstone (Sakinç et al. 1999; Duman et al. 2004). The sites of all the landslides occurred on the Miocene deposits are confined by the coastal region (Fig. 3).

The activity of the WBSF that continued from Cretaceous to Mid-Eocene was ended by the collision of the Istanbul Zone with the Sakarya continent in mid-Eocene (Okay et al. 1994). In addition, Eocene sedimentation indicating some dip-slip activity during the Middle to Late Eocene is controled by the Çatalca Fault Zone. The active NAF passes ca. 10 km of the coast (Okay et al. 1999; Le Pichon et al. 2001) forming an east–west-trending segment about 110 km long. According to Barka and Hanckok (1985) and Aksu et al. (2000), it has been active since the Late Miocene–Pliocene. This study indicates that thin blanket of Pliocene/Quaternary deposits are underlain by older strata of Miocene and Oligocene characterize the northern shelf area. The older strata cut by various order of faults are usually parallel layered with gentle slopes.

Generally considering the study conducted on this new branch of the NAFZ in the Marmara Sea, seismic, morphological and sedimentological data obtained in this area

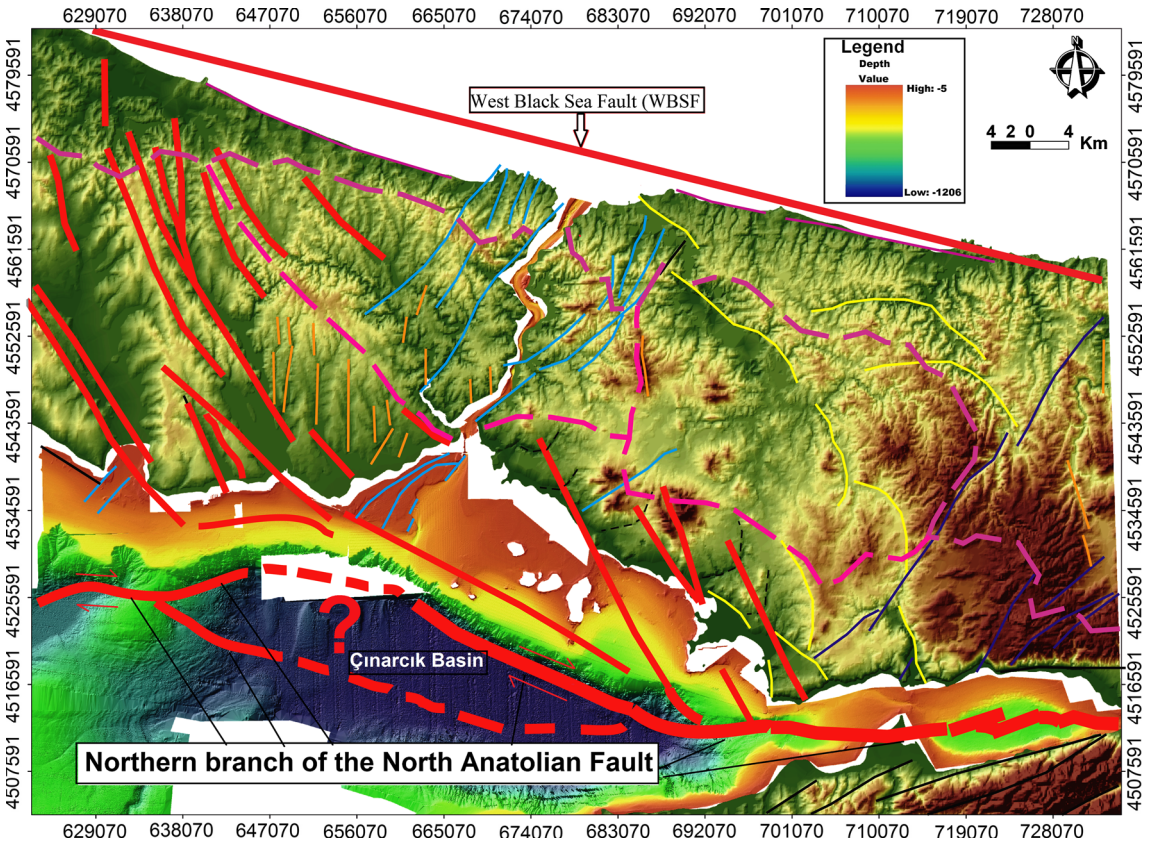

Fig. 4 Marmara Sea bathymetric data and the lineaments in Istanbul and Kocaeli Peninsulas

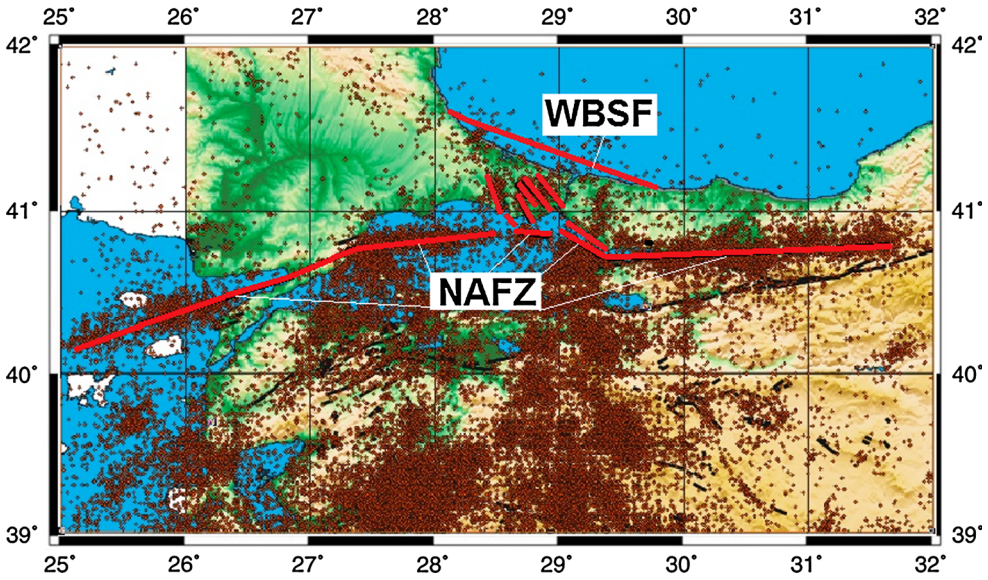

Fig. 5 Epicentral distributions of the earthquakes recorded by the Kandilli Observatory from 1900 to 2013. (The map was taken from Bogazici University Kandilli Observatory and earthquake Research Institute seismology Laboratory)

indicate that the fault along the western part of the Marmara Sea consists of a single main fracture (Figs. 4, 5). Similar data show that the NAFZ continues into the Çınarcık Basin as a single fault zone across the middle axis of the Gulf of İzmit (Gürbüz et al. 2000; Okay et al. 2000; İmren et al. 2001; Gökaşan et al. 2001, 2003; Le Pichon et al. 2001; Gazioğlu et al. 2002; Kuşçu et al. 2002). Some problems are still debated, such as the fault geometry within the Çınarcık Basin and the number of its branches (Fig. 4).

Detailed morpho-tectonic assessment of the multibeam data collected by the Turkish Navy, Department of Navigation, Hydrography and Oceanography for the bottom of the Marmara Sea has shown significant differences between the northern and southern slopes of the deep basin (Gazioğlu et al. 2002). The most remarkable morphological difference between the slopes is that the northern slope has higher gradients than the southern one (Fig. 4). This analysis has also revealed that the northern slope is divided into two different morphological groups including high-inclined linear slopes and relatively lower-inclined concave slopes. Thus, since the steep and linear slope at the north of the Çınarcık Basin has younger formations morphologically, it has been concluded that it has a retreated surface compared to other concave slopes. This linear morphology suggests that this slope is controlled by a strike-slip fault. Three aftershocks occurring on this slope after the Earthquake of 17th August are supporting this morphological interpretation (Orgülü and Aktar 2001).

Some studies have evidenced that the NAFZ passing through the Gulf of İzmit follows the northern slope or the middle axis of the Çınarcık Basin and is linked to the fault at the west (İmren et al. 2001; Gökaşan et al. 2002, 2003; Yaltırak 2002; Fig. 6a, d–f), other studies have shown that the fault follows the northern slope of the Çınarcık Basin (Okay et al. 2000; Le Pichon et al. 2001; Rangin et al. 2004; Sengör et al. 2005; Fig. 6b). Even though Le Pichon et al. (2001) and Gökaşan et al. (2002; 2003) present different interpretations, İmren et al. (2001) have suggested that the northern slope of the Çınarcık Basin is controlled by a strike-slip fault (Fig. 6a, b, e, f). The same slope has been interpreted as a normal fault by Yaltırak (2002) and Armijo et al. (2002, 2005) (Fig. 6c, d). On the other hand, Le Pichon et al. (2001); (Fig. 6b), Demirbağ et al. (2003) and Rangin et al. (2004) have shown that there is no branch following the southern slope of the Çınarcık Basin.

The interpretative differences in the tectonic models produced for the NAFZ in the Marmara Sea mainly regard the active kinematic of the fault in the Çınarcık Basin. While this can be considered that the studies have reached an important stage, since the debated area is right at the south of Istanbul, obscurity of hazards to this important city has not decreased. Therefore, solution to the geological problems in the Çınarcık Basin and its surroundings maintains its importance with an increasing priority compared to the other areas of the Marmara Sea. The active tectonics in this area is not still clear because the Çınarcık Basin and its surroundings have a highly complex geological structure, as well as because Quaternary geological processes in the adjacent Çatalca and Kocaeli Peninsulas are known only to a very limited level.

Morphological setting

The morphological lineaments, some of which are defined as faults, situated on İstanbul and Kocaeli Peninsulas show conformity with the NW–SE extension of the NAFZ within the Çınarcık Basin (Fig. 4). A mature erosional surface and the southwestern edge of the Strandja Mountains are included major morphological properties on İstanbul Peninsula. The erosional surface cut by rejuvenated streams (Fig. 7a) has been dated as Upper Miocene-Upper Pliocene since the twentieth century (Cvijic 1908; Chaput 1936). The largely parallel drainage patterns of the major valleys developed on Miocene rocks, and lattices on Paleozoic rocks (Erinç 2000). There are also variety of shorter NE–SW extended lineaments between the NW–SE oriented lineaments are cut by NW–SE ones (Gökasan et al. 2002; Fig. 7a–f). A rejuvenated morphology with linear scarps is also presented by the Strandja Mountains (Fig. 7a). The scarps and drainage system generally show a NW–SE direction (Fig. 7a). During the assessment of the unexpected effect of the earthquake on Avcılar, this similarity was considered, and many morphological elements in the same direction as the fault in the northern slope of the Çınarcık Basin were reckoned with in the morphology of Istanbul Peninsula (Gökaşan et al. 2002; Fig. 7a–f).

Lineament L1 can be observed from the east of İstanbul Strait to the west of the Terkos Lake. The NW–SE-oriented linear Marmara Sea shoreline on the Kocaeli Peninsula and the Golden Horn are considered as the eastern edge of L1 (Fig. 7b). L1 follows the northern scarp of the Derbent Hill, and the source of the Alibey Stream then it passes through the Terkos Lake and units with lineament L2 on the Black Sea coast of the Thrace Peninsula (Fig. 7b–f).

Indicators of lineament L2 are the NW–SE central axis of the Küçükçekmece Lagoon and the 3.5 km long right-lateral displacement on the Marmara Sea coast of the lagoon (Fig. 7a–d). L2 that passes through a right-lateral displacement in the watershed between the Koğukdere and Sazlıkçayırdere streams extends northwards following the NW–SE valley of the Koğukdere Stream (Fig. 7a, b, d), and follows the western side of this watershed (eastern side of Sazlıkçayırdere Stream) to the north (Fig. 7a–d). The northern extension of L2 is formed by scarps along the northeastern edge of the Strandja Mountains (Fig. 7a, b, d, e). L1 joins to L2 on the Black Sea coast in the northern sector of these scarps. L2 passes through a right-lateral displacement on the Black Sea shoreline (Kıyıköy Peninsula), and it extends along the southern edge of the İğneada Bay to the NW corner of the study area (Fig. 7a, b, d, e).

The southernmost extension of lineament L3 is represented by right-lateral displacement on the Marmara Sea shoreline (Fig. 7a, b). The course of lineament L3 is indicated by the

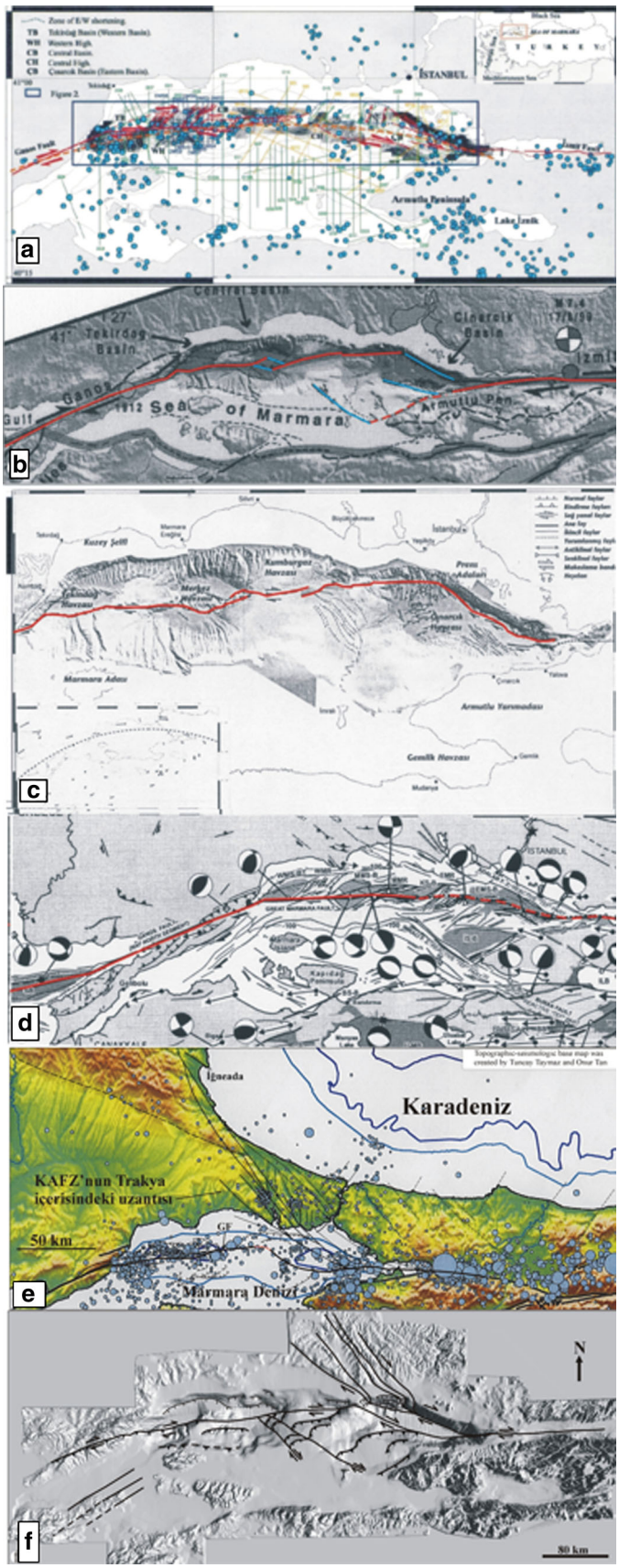

Fig. 6 Some of the active fault models in the Marmara Sea as the result of the use of the detailed bathymetric data [Imren et al. 2001 (**a**); Armijo et al. 2002 (**b**); Le Pichon et al. 2001 (**c**); Yaltirak 2002 (**d**); Gökasan et al. 2002 (**e**); Gökasan et al. 2003 (**f**)]

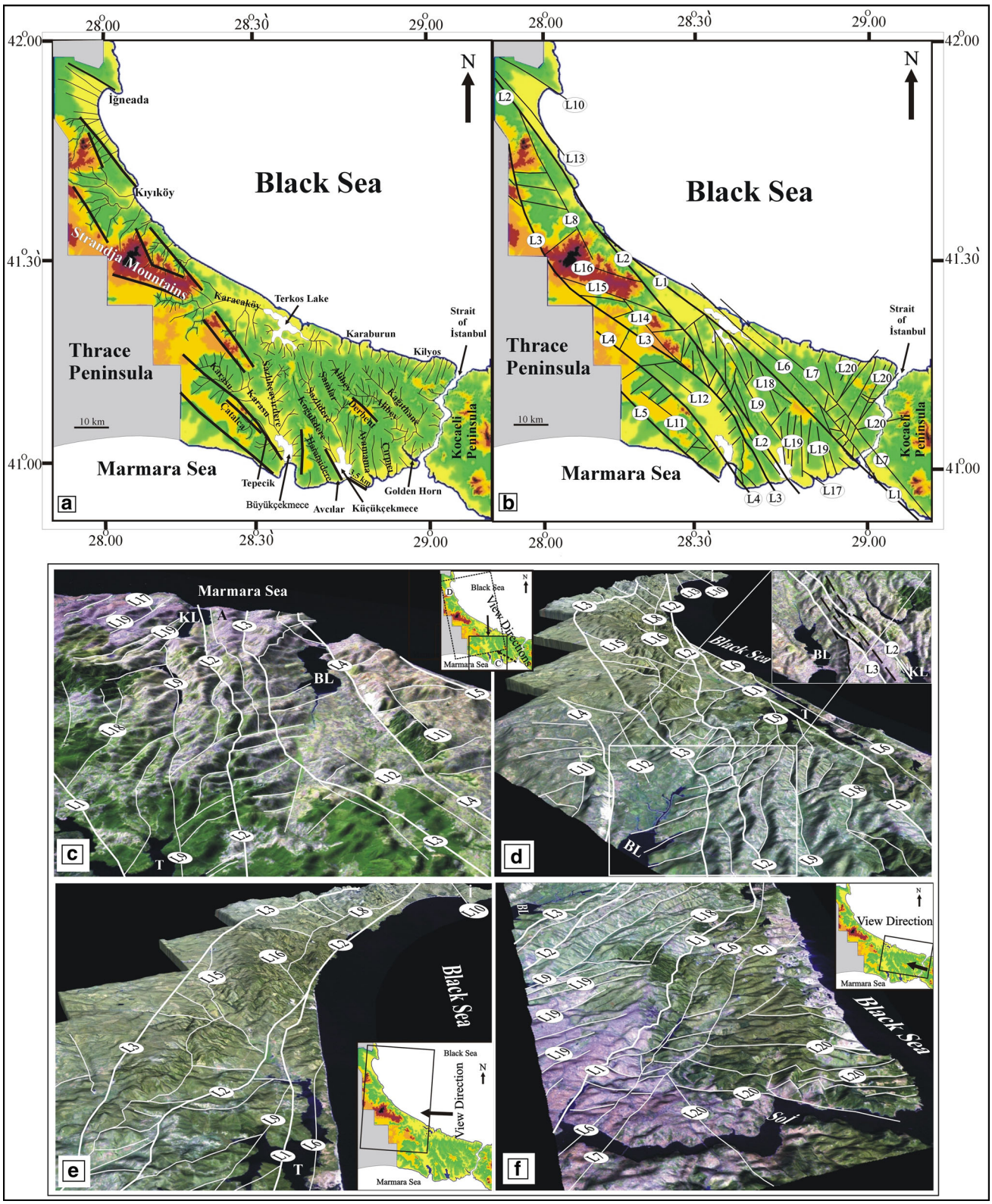

Fig. 7 Digital terrain models for Istanbul Peninsula and their interpretations (Gökasan et al. 2002)

NW–SE Haramidere stream valley and the eastern side of Büyükçekmece Basin (Fig. 7a–e). This lineament passes through a right-lateral displacement in another watershed between the Haramidere and Sazlıkçayırdere streams (Fig. 7a, b, d). The southwest facing scarps of the Strandja Mountains discloses the northern extension of L3.

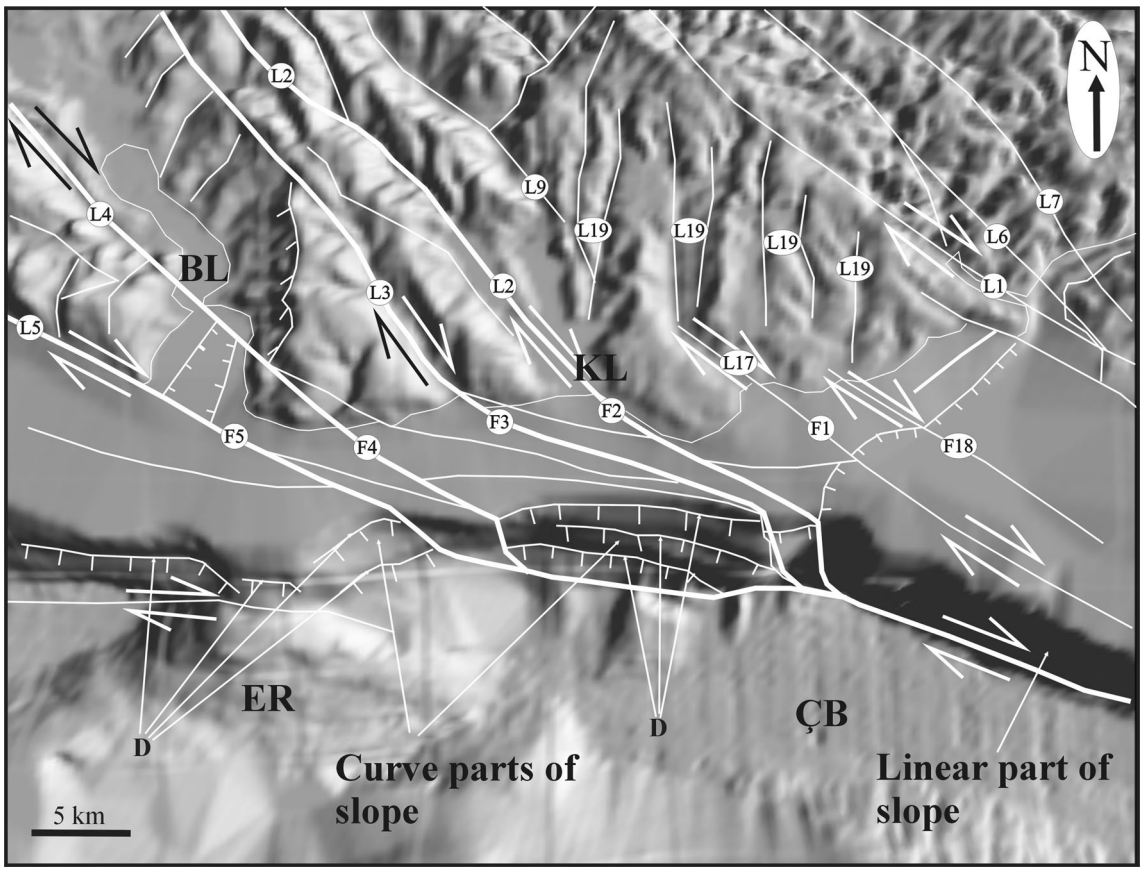

Fig. 8 Digital terrain model and lineaments between the Istanbul Strait and Büyükçekmece Gulf. Faults (*F*) cutting the sea floor of and lineaments on land (*L*) aligning with the faults *BL* Büyükçekmece Lagoon, *KL* Küçükçekmece Lagoon, *ÇB* Çınarcık Basin, *ER* Eastern Ridge, *D* dip-slip movement caused by sub-marine landslides and normal faults (Gökaşan et al. 2002)

Lineaments L4 and L5 are revealed by the north and south facing scarps of the Çatalca Rise (Fig. 7a, d). The alignment of L4 is followed by the southwestern side of the Büyükçekmece Basin and the Tepecik stream valley. Lineaments L6 and L7 are parallel lineament L1 in the north of the study area (Fig. 7a, b, d–f).

In the north of the study area, lineaments L6 and L7 show parallel features to lineament L1 (Fig. 7a, b, d–f). L6 starts from the southern entrance of the İstanbul Strait and follows the Alibey stream valley and the northern shoreline of Terkos Lake to lastly passes through the right-lateral displacement on the Black Sea coast of the Thrace Peninsula. L7 extends from the Kocaeli Peninsula in the east from where it crosses the Bosphorus, passes through the Kağıthane Stream valley to cut the Black Sea coast northeast of Terkos Lake (Fig. 7b, f).

Lineament L8 merges with L2 where they meet the northeastern slope of the Strandja Mountains (Fig. 7a, b, d–e). Lineament L9 conforms to the Sazlıdere stream valley (Fig. 7a–f). Lineament L10 is assesed as a right-lateral displacement along the northern shoreline of İğneada Bay (Fig. 7a, b, d–e). Lineaments from L11 to L18 describe the shorter NW–SE oriented lineaments depicted in Fig. 7a–f.

The offshore part of the lineaments labeled as L in Fig. 4 is composed of the linear NW–SE aligned northern slope of the Çınarcık Basin. A NW–SE oriented linear offshore slope is formed by this lineament that is located between the Marmara entrance of İzmit Bay and the southeastern shore of Küçükçekmece Lagoon. This linear slope curves into an E–W direction to the south and southwest of Küçükçekmece Lagoon (Fig. 4).

Some of these lineaments are the onshore traces of the faults and those can be recognized by seismic data offshore Avcilar in continuation of these lineaments on land (Gökasan et al. 2002; Figs. 8, 9). According to the bathymetric data collected by R/V Le Suroit Research Vessel, there is a relation between the NW–SE- right-lateral ruptures sighted in the northern slope of the Çınarcık Basin for the SE-continuation of these faults (Fig. 10). As a conclusion, the fault following the northern slope of the Çınarcık Basin and the main branch at the west do not join. The fault needs to go landward as a secondary branch of

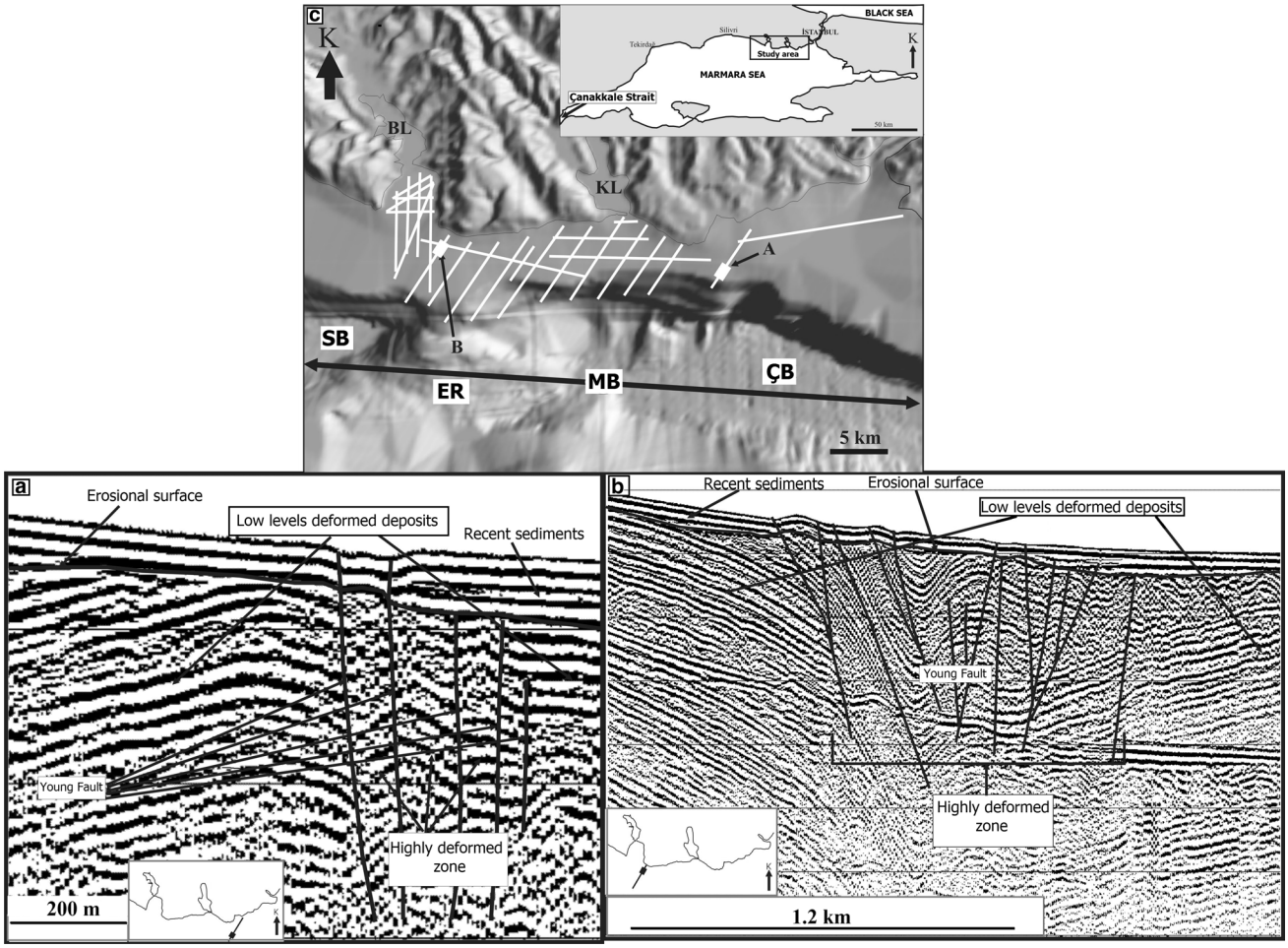

Fig. 9 Young faults observed on seismic profiles collected at offshore areas of Avcılar (Gökaşan et al. 2002)

the Trakya Fault (Perinçek 1991) reactivated by the NAFZ. The main fault of the NAFZ follows the southern slope of the Çınarcık Basin (Gökaşan et al. 2002). According to the morphological explication, a similar fault needs to control the NW–SE-shoreline between the Istanbul Strait and Tuzla.

To summarize, previous seismic, morphological and sedimentological studies about the Istanbul Strait reveal the existence of some young faults, whose effects have been observed on the sea bottom along the Istanbul Strait and its exits at the north of the Çınarcık Basin (Alavi et al. 1989; Yılmaz and Sakınç 1990; Yıldırım et al. 1992; Gökaşan et al. 1997; Gökaşan 2000; Demirbağ et al. 1999; Oktay et al. 2002). The existence of some young faults on onshore extensions of the faults observed at sea has been determined by field studies (Meriç et al. 1991a, b; Koral and Şen 1994). The faults forming the İstanbul Strait were controlled by a counterclockwise rotation of the area between the NAFZ northern branch passing through the Marmara Sea (Oktay et al. 2002) and the fault is asserted to exist on the Black Sea coast by Demirbağ et al. (1999). In the light of multibeam and seismic data obtained from the Turkish Navy, Department of Navigation, Hydrography and Oceanography (TN-DNHO), the bottom of the İstanbul Strait is mainly controlled by erosional processes (Gökaşan et al. 2005) and interrupted by some faults of which effects reach to the sea bottom (Gökaşan et al. 2006). In the northeastern shelf of the Marmara Sea, seismic and bathymetric data show that secondary faults are NW–SE and NNE–SSW oriented (Tur 2007). Ergintav et al. (2011) reveal that because of the stress field of the active tectonic regime, the faults located in the Istanbul Strait have been reactivated as secondary faults.

Materials and methods

In this study, in the northern shelf of the Marmara Sea, multibeam bathymetric and seismic data collected by the Turkish Navy, Department of Navigation, Hydrography and Oceanography (TN-DNHO) were processed. In addition to these data collected offshore, digital topography

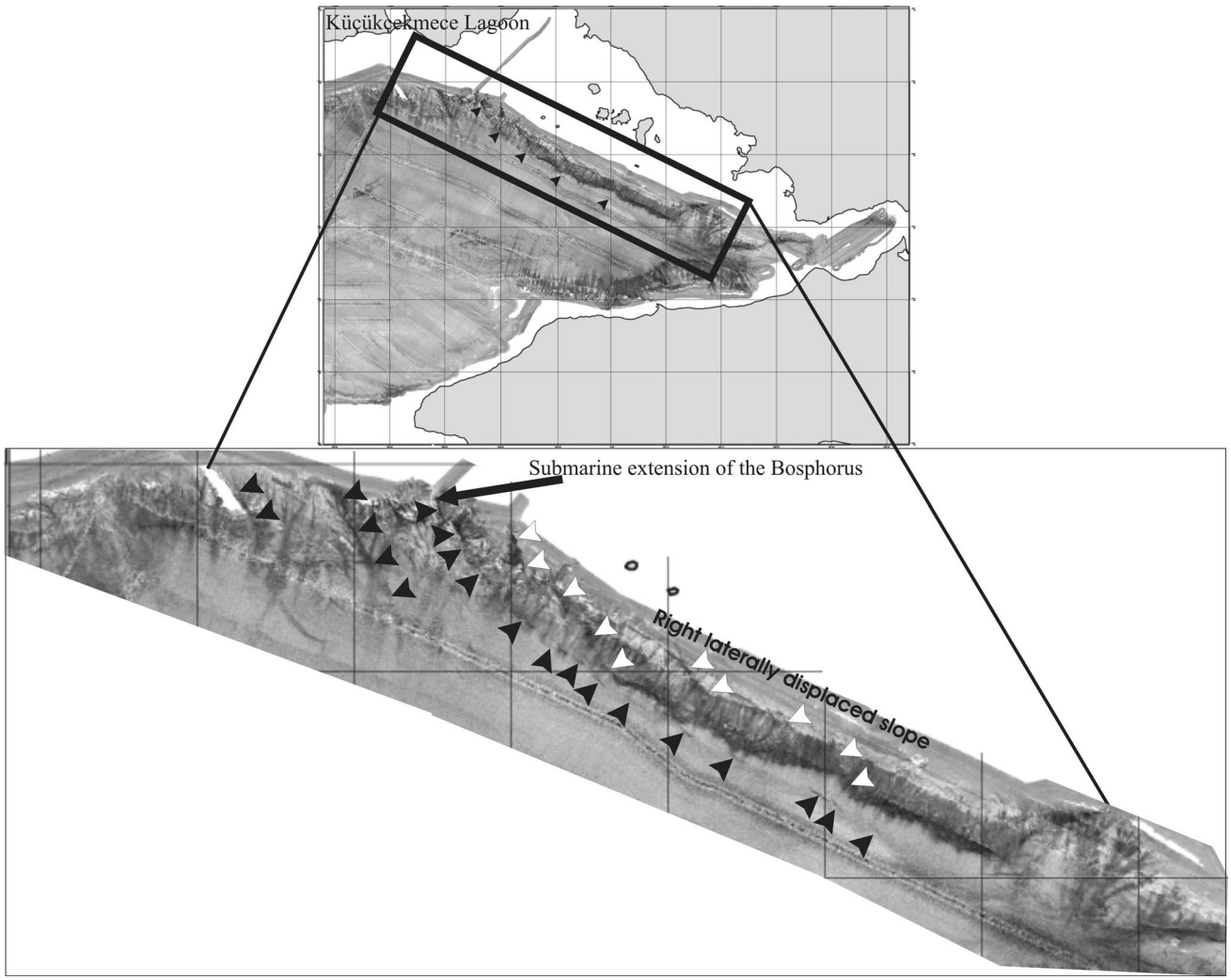

Fig. 10 Fault model suggested for the northern slope and the northern shelf of the Çınarcık Basin (Gökaşan et al. 2002)

data of land area were combined with bathymetric data. Digital terrain model of around the study area was created with this way.

Bathymetric–topographic data

As a general evaluation, this method is known as the best of the seafloor mapping techniques, since imaging seafloor at high resolution is possible using multibeam bathymetric data. In this way, the microbathymetry of sea floor can be mapped at the high resolution (±5 cm). These images, known as digital terrain imaging, are superior in terms of information richness in details to bathymetric maps based on point measurements. Bathymetric data were collected by using a system that can reach up to 120° scanning angle. The system contains 56 cyrstal cells and provides continuous search up to 700 m by using 180 kHz and up to 2,500 m by using 50 kHz. Transducers of Elac-Nautic 1050 D multibeam sonar are set up to the bottom of the vessel. Produced 56 U ray can be transmitted as 120° form of fan in the Çubuklu vessels. In the Mesaha-2, these values are 126 U and 153°. In this study, data obtained from UTM-35 projection WGS-84 coordinate system by using Mesaha and TCG Çubuklu vessels were used. The vessels belong to the Turkish Navy, Department of Navigation, Hydrography and Oceanography (TN-DNHO). Since depth measurement system is set up to bottom of the ship, the vibration caused by the ship's engine was recorded. When this effect drew less attention in the contour maps containing colour code, short wavelength undesireable structures displaying continuity at the direction of movement of the ship occur in the shaded maps that are used to image structural elements. The noise partially covers the structures and makes interpretation difficult. Short-wavelength noises are filtered in the desired range by using developed low-pass filtering techniques so optimum

filtered maps reveal real morphology of the sea floor and enable the user to select details easily. These data were tranferred to Er Mapper program as Binary grid and combined with topography data in order to obtain a digital terrain model of the study area.

Seismic data

Seismic data used in this study were collected in previous years by the Department of Hydrography and Oceanography (TN-DNHO) by using 230 Uniboom shallow system and Sparker shallow seismic system. Uniboom anolog system consists of seismic energy unit (300 J), transducer, single hydrophone streamer and analog recorder. Energy supply is used by Uniboom seismic transducer supplied with 110 or 220 VAC. The supply voltage is converted to 3.5 KVDC by means of transformators of transducer. Capacitors are charged by this DC current. It contains 3 pieces 100 J capacitors. These three capacitors are connected as parallel with each other, 100, 200, 300 J of energy can be obtained. Model 230-1 Uniboom sound source is the acoustic device that converts electric energy to sound energy. The device mounted on a catamaran consists of coil and plate. Once decharging energy stored at the source into the sea over the coil, the plate connecting with springs is pushed. Once the plate is back into previous position, an acoustic plus is created. The frekans ranges of an acoustic puls are 700–14,000 Hz for 100 J, 500–10,000 Hz for 200 J, 400–8,000 Hz for 300 J. The task of Model 265 hydrophone is to transfer acoustic pulses reverberating from bottom layers of sea into the recorder. It consists of two coils as active portion and cable. Active portion contains 8 U piezoelectric crystal in kerosene and preamplifier supplied by 9 volts DC current. Frekans range is between 400 Hz and 5 kHz. The compression in active portion created by acoustic pulses reverberating from bottom layers of sea converted by means of piezoelectric crystal. This very low current is transmitted to the recorder via preamplifier. A sparkarray system is used to determine thickness of the sediment on the sea floor and the features of the main rock. It is operated from the surface and it collects analog data. In the case of using additional power units and capacitor, it can be used up to 8,000 J. Sparkarray seismic reflection system consists of following items. Model 232-A, power supply, provides charging of capacitors by creating 3.5-4 KVDC current. Model 233-A, a capacitor bank, stores 2,000 J energy. It contains 20 pieces parallel connected capacitors (each 100 J, total 2,000 J). Model 231 contains 10 pieces parallel connected capacitors (each 100 J, total 1,000 J) and contains trigger circuit that is supplied with 110 volt power. Model 255-8,300, recorder, is designed with together Uniboom system and Sparker system. It has the ability to expand seismic waves and to scroll above or down. It can provide discharging of energy source in desired range. In device, there are 50–2,000 Hz cutting filter and TGV and threshold that eliminate at least 60 db noise. In case of using with magnetic recorder that contains double channels, it provides better-quality recording.

Results

Interpretation of the multibeam bathymetric data between the Istanbul Strait and Büyükçekmece Gulf Shelf area

The geological interpretation of multibeam data collected in the northern shelf of the Marmara Sea remaining between the Istanbul Strait and the Büyükçekmece Gulf for the area of study, have evidenced the occurrence of almost horizontal sea bottom morphology, deepening with low angles up to about 100 m (Fig. 11). This uniform morphology is interrupted by tectonic and morphologic lineaments parallel with the shoreline around the Istanbul Strait and the Küçükçekmece Lagoon (Fig. 11). In addition to these, two significant canyons observed at the periphery of the shelf at offshore parts of the Büyükçekmece Lagoon indicate a significant sediment transfer occurring along the slope in this area (Fig. 11).

Showing more in detail, in Fig. 11, a lineament occurring at −25 m water depth has been observed and compared with the Bosporus Canyon which has a depth of −65 m between the western slope and the shore line of the Bosporus (Fig. 11c). This lineament appears to be the submarine extension of the land area behind based on its morphology. Moreover, the top of this lineament which has a shallower depth than the overall depth of the shelf is highly irregular. This irregularity represents itself a wide depression formed by merging of NNE–SSW oriented local concavities observed throughout the area in question (Fig. 11a). The northernmost one of these concavities in the depression is observed to form a canyon in this area by interrupting the western slope of the strait (Fig. 11c). Based on its morphology, this canyon and the concavity behind it can be interpreted as a river valley having impact on this area and a canyon where this river joined the strait when the sea level was about 90 m deeper than its current level during the last glacial period (Smith et al. 1995). Nevertheless, linear slopes and arrays of these concavities indicate that they were also affected by structural elements. Then, the array of these concavities shows that each of them forms a NNE–SSW-lineament (L1) at the sea bottom. In this area, similar linearities observed at the western slope of the Bosphorus Canyon are interpreted as NNE–SSW-benches controlled by the fault n. 12 (illustrated in

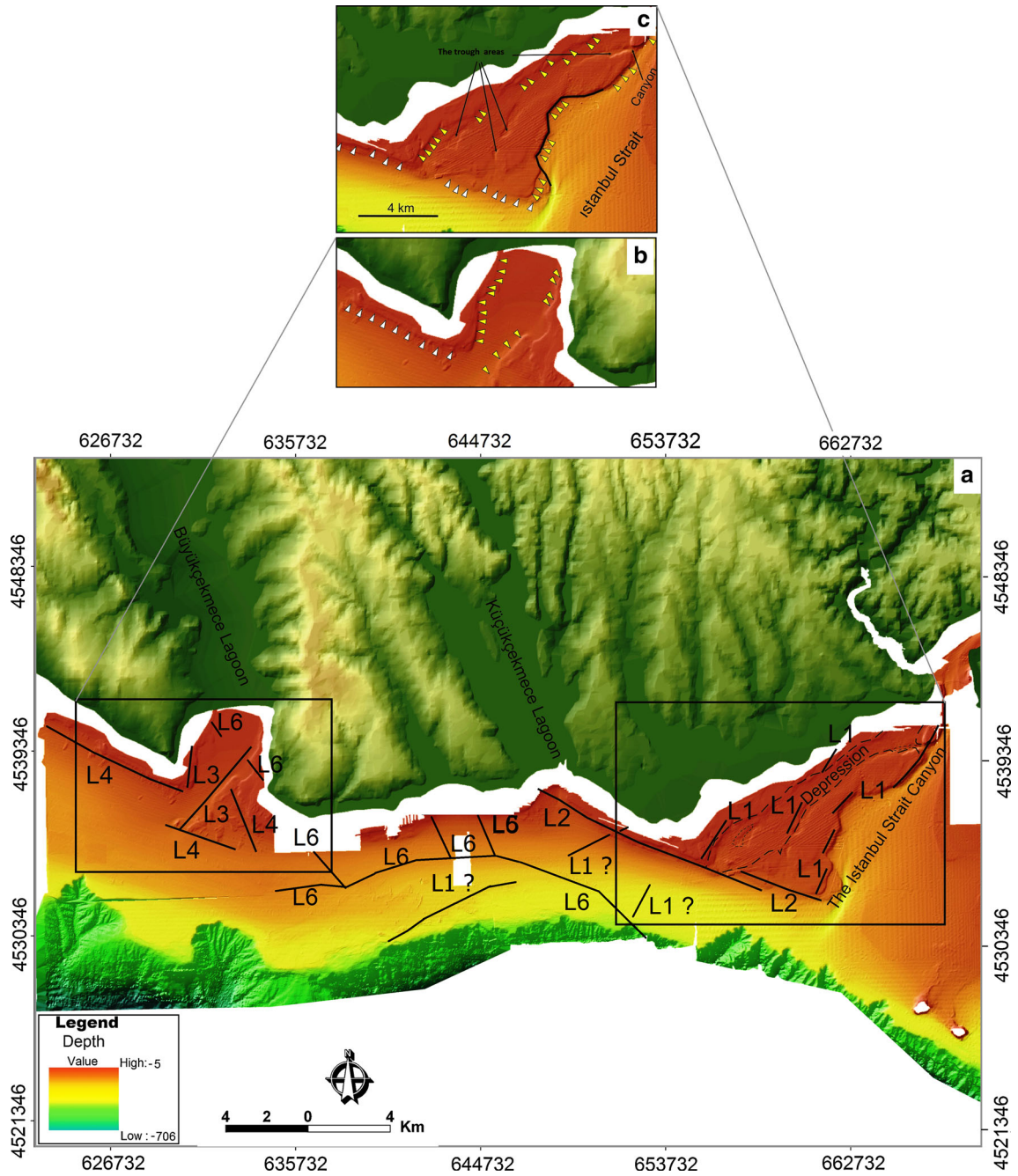

Fig. 11 **a** Lineaments in bathymetric map of the shelf area from the Strait of Istanbul Canyon to Büyükçekmece Lagoon. **b** Detailed multibeam bathymetric maps for the offshore parts of Büyükçekmece. **c** Detailed multibeam bathymetric maps for the western slope of the Istanbul Strait

Fig. 21a, Tur 2007) in the seismic interpretations made for the eastern part between the Gulf of Tuzla and the Bosporus in the study (Fig. 11c). The western slope of the strait controlled by the mentioned fault presents a complex slope morphology consisting of NNE–SSW-linear slope pieces. Since this slope actually has a concave morphology opening towards the strait canyon in general although consisting of linear slope tracts (Fig. 11c), we also consider that a landslide could have an effect on the slope other than the faults. As the seismic studies conducted in this area assert that the sedimentary mass in the strait canyon can be slipped material from a landslide (Gökaşan et al. 2004), it supports this interpretation. A NW–SE-slope forms the southern border of this high plain located between the western slope and the shore line of the Bosphorus (Fig. 11c). This linear slope indicates existence of a NW–SE-lineament (L2). The westward continuation of this slope unites with a bench at the offshore parts of the NW–

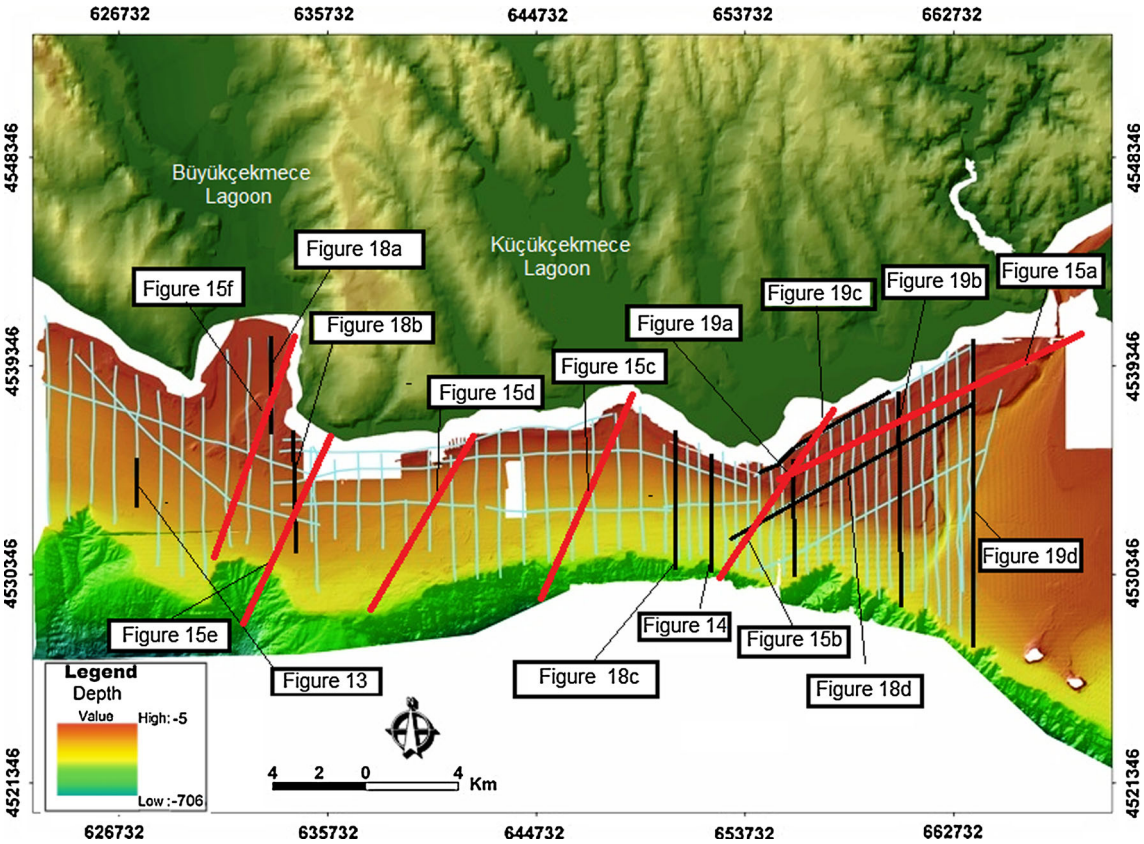

Fig. 12 Seismic profile map of the Istanbul Strait Canyon-Büyükçekmece Gulf in the shelf area

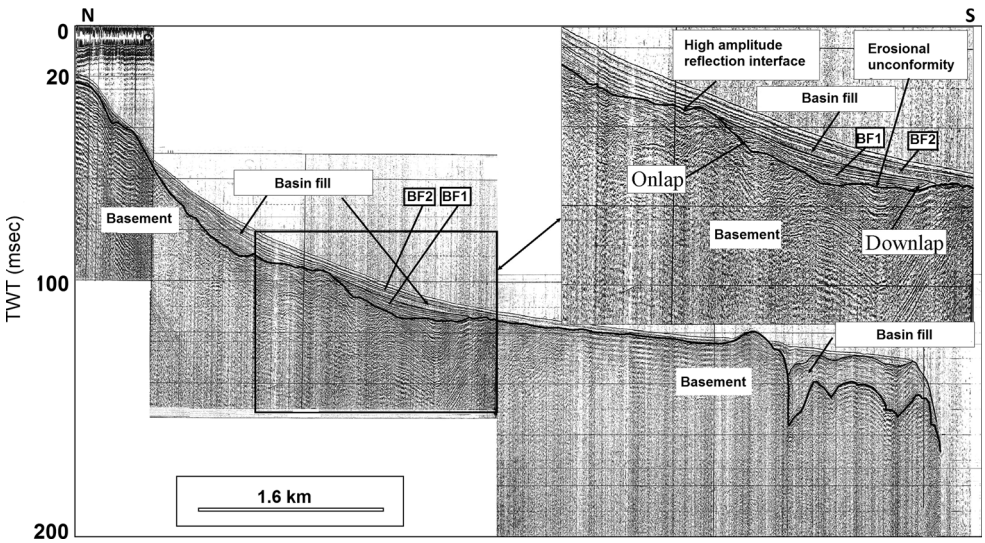

Fig. 13 Stratigraphic interpretation of a seismic profile of the west of Büyükçekmece Gulf on the Marmara Sea Shelf; see Fig. 12 for the site location

SE-linear shore line at the east of the Küçükçekmece Lagoon and at the sea bottom in parallel with it (Figs. 10, 11c). In the area where this lineament ends at the east, existence of an N–S-narrow and deep channel leaning on the west slope of the Istanbul Strait Canyon draws attention. This channel may either be formed by the undercurrent in that area or developed by the effect of a young structural element in that area on the sea bottom.

In this area, the second area with a complex morphology on the shelf is seen at offshore parts of the Büyükçekmece Lagoon (Fig. 11a, b). Elements causing the complexity on the shelf in this area are the submarine continuations of the

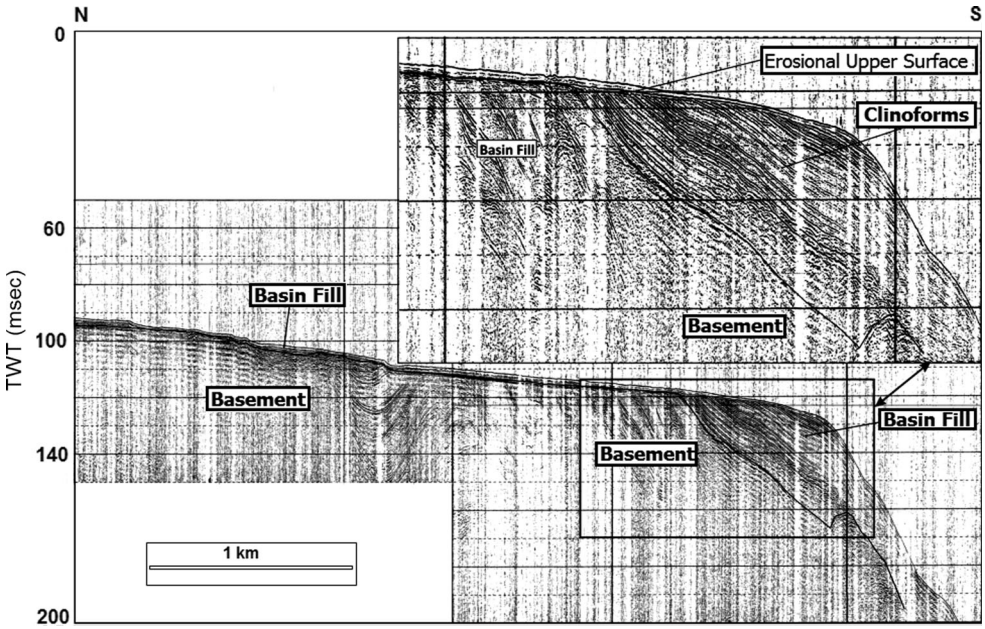

Fig. 14 Stratigraphic interpretation of a seismic profile of the east of Küçükçekmece Gulf; see Fig. 12 for the site location

land pieces bordering the Büyükçekmece Lagoon at the east and the west. Benches formed by these borders at the sea bottom form the N–S and NNE–SSW-lineaments in this area (L3, Fig. 11b). These benches observed on the shelf bottom are bordered by the NW–SE linear benches lying under the sea in line with the general trend of the shore line. These benches observed under the sea are interpreted as NW–SE-lineaments having effect on this area (L4; Fig. 11b). Lineaments observed at offshore areas of the shore line between Küçükçekmece and Büyükçekmece are called as L5 (Fig. 11a). Additionally, lineaments (L6) directed SW-NE are recognized from digital land topographic map.

Seismic interpretation

Seismic data from the shelf area of the Küçükçekmece and Büyükçekmece Lagoons were interpreted stratigraphically and structurally by tracing the submarine continuation of the lineaments onshore.

Seismic stratigraphy

Seismic profiles (Fig. 12) collected by the single-channel sparker and boomer seismic data acquisition system at the shelf area between the İstanbul Strait Canyon and the Büyükçekmece Gulf have been reinterpreted in this study. The location map of seismic profiles, superimposed on the marine DEM, is shown in Fig. 12.

Three sediment sequences and a truncation are distinguished using the reflection configuration of the sediment deposits. These sequences are named lower unit, upper unit, and deltaic sequence. Although reflection configuration of the lower unit indicates a characteristic deformation, its initial internal parallel reflectors are observed on the seismic profiles. An angular unconformity marks the top of the lower unit, indicating an erosional period after deposition.

Lower unit (*acoustic basement*) in the study area it has been observed that the lower unit has a surface with high reflection amplitude (Fig. 13). This surface indicates that the acoustic impedance difference between the lower unit and the overlying unit is high. This in turn indicates a significant physical distinction between the lower unit and the upper one, respectively composed of rock and sediments. The upper border of the lower unit suffered from erosion in this area as well (Fig. 13). Top surface of this unit ends with onlap and downlap of reflection surfaces of the sediments in the Upper Unit (Fig. 13). It indicates that the Lower Unit must be an acoustic basement for the sediments on it same as in the eastern part of the area of study. Since the top surface of the Lower Units gets shallow towards the land, it suggests that this surface unites with the top surface of widely exposed units on land (Fig. 13). As Oligocene and Upper Miocene units outcrop at the Marmara Sea coast in the İstanbul Peninsula, in the part remaining between the Bosporus and the Büyükçekmece Lagoon (Fig. 14), the units constituting the acoustic basement observed in seismic profiles probably consist of Oligocene and Upper Miocene units. With a similar approach in previous studies conducted in the area, this unit has been interpreted as the submarine continuation of Oligocene–Upper Miocene-aged units (Gökaşan et al. 2002; Oktay et al. 2002). Therefore, we conclude that the

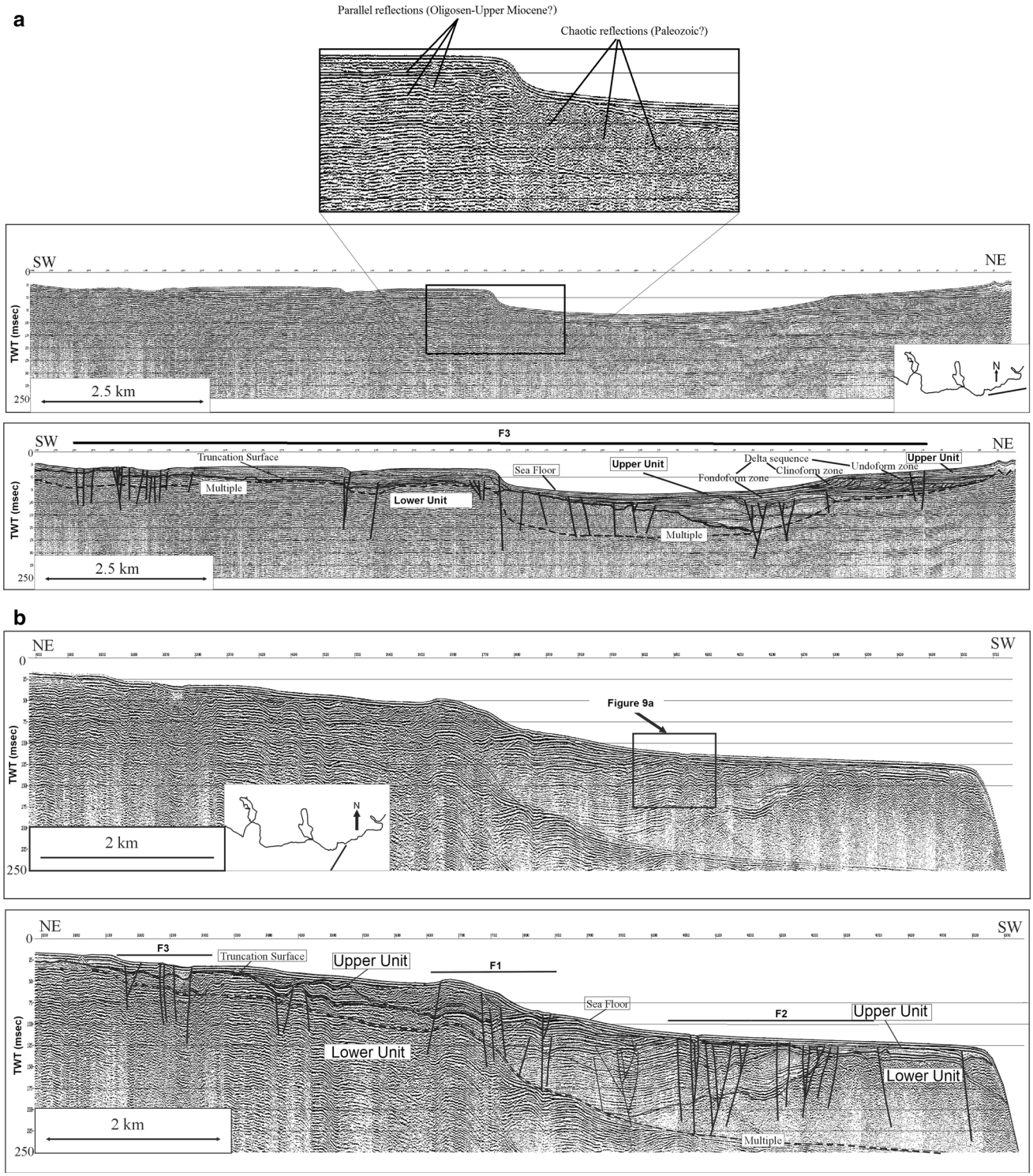

Fig. 15 **a–f** Stratigraphic and structural interpretations of seismic sections. Detailed explanation of the possible faults given in the text (modified from Gökaşan et al. 2002)

unit below the high amplitude reflection surface in seismic profiles (Lower Unit) is the submarine continuation of the Oligocene–Upper Miocene aged stack outcropping in wide areas along the Marmara Sea coast in Istanbul Peninsula. The seismic facies of the lower unit varies from chaotic to parallel. The reason for difference of this reflection formation from the Paleozoic-aged Lower Unit between the Gulf of Tuzla and the Bosporus is that the Oligocene-

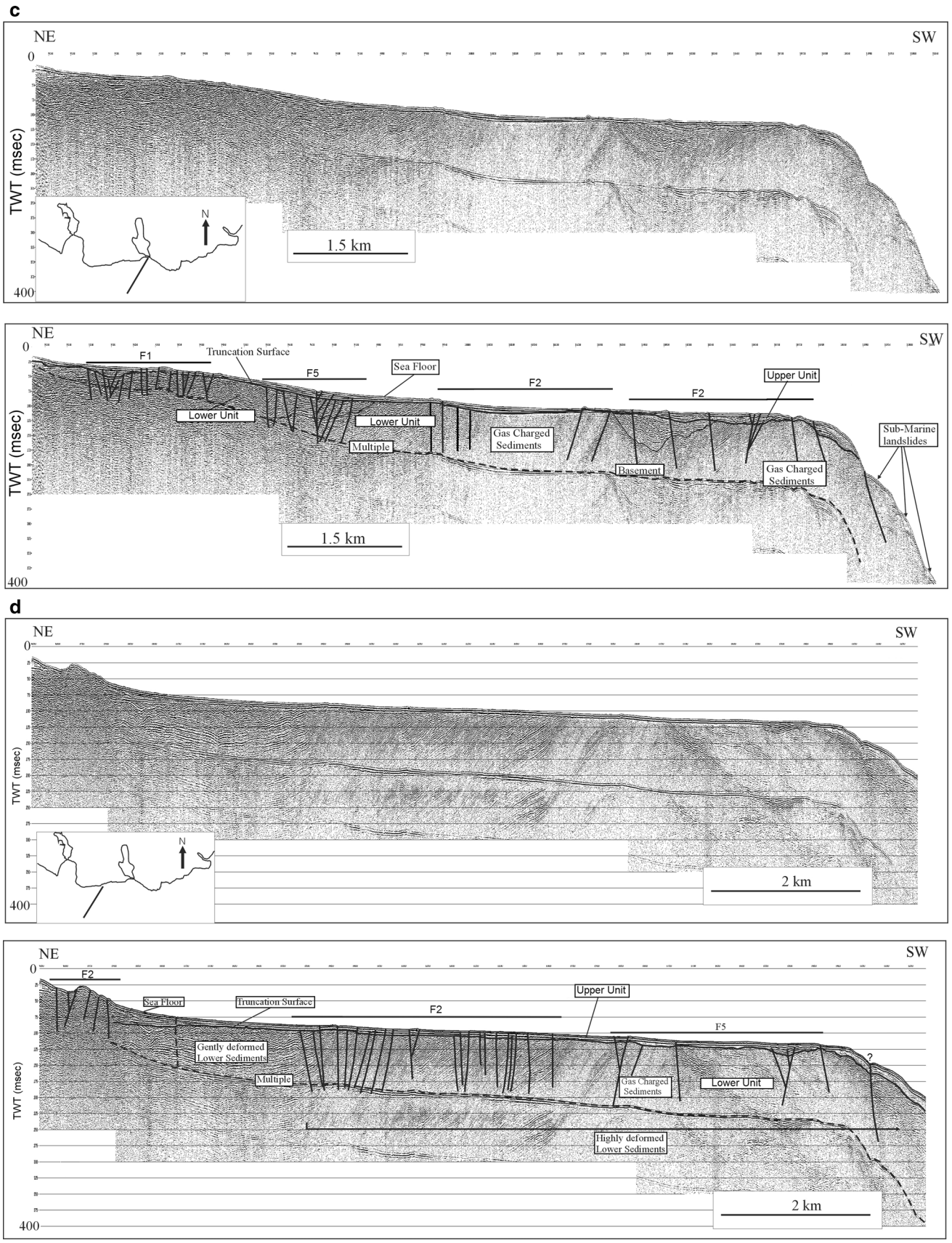

Fig. 15 continued

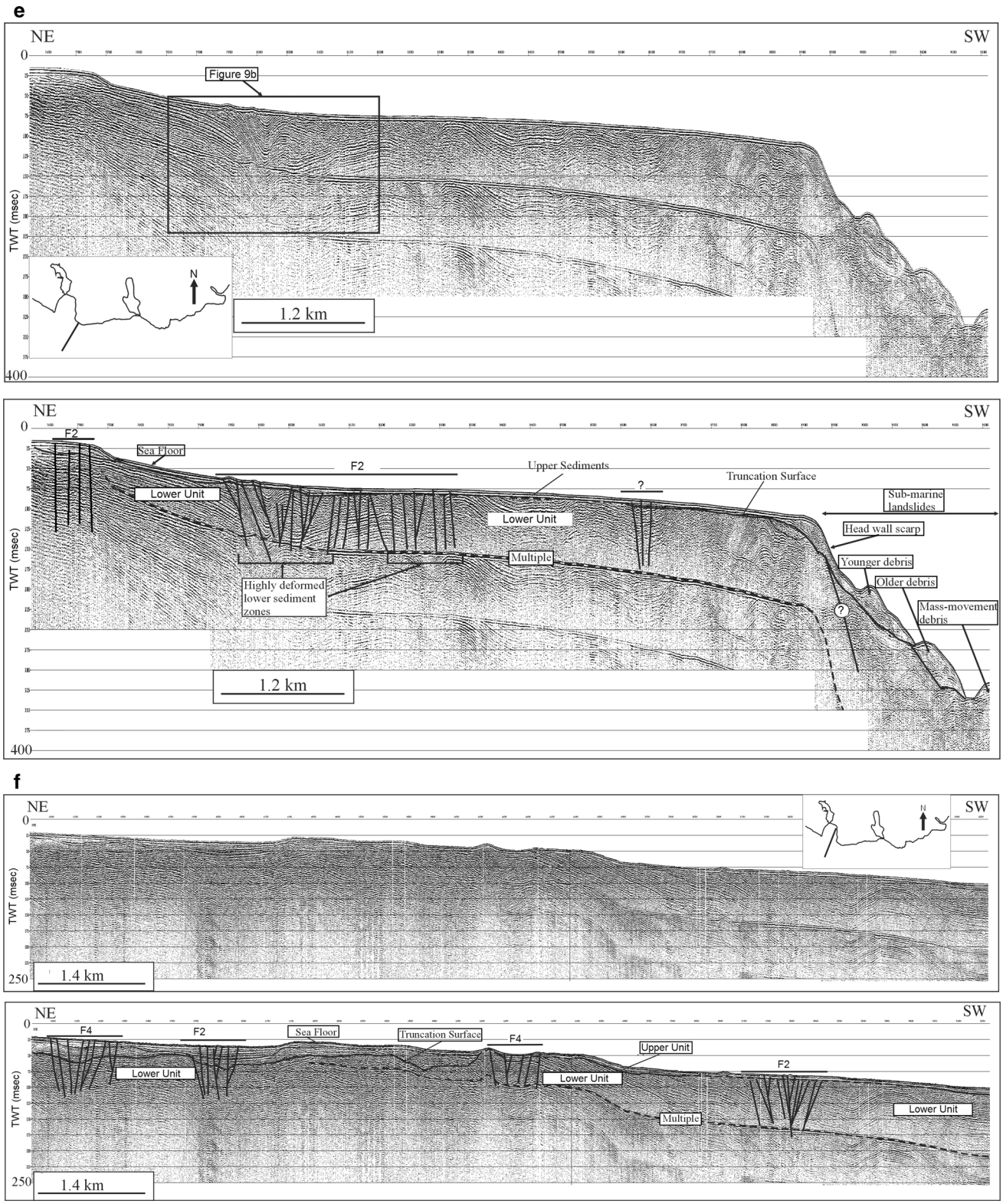

Fig. 15 continued

Upper Miocene aged acoustic basement underwent much less deformation compared to its Paleozoic-aged counterpart at the east due to the significant age gap between the units and thus it maintained its layer structure in the primary depositional environment to a certain extent (Tur 2007).

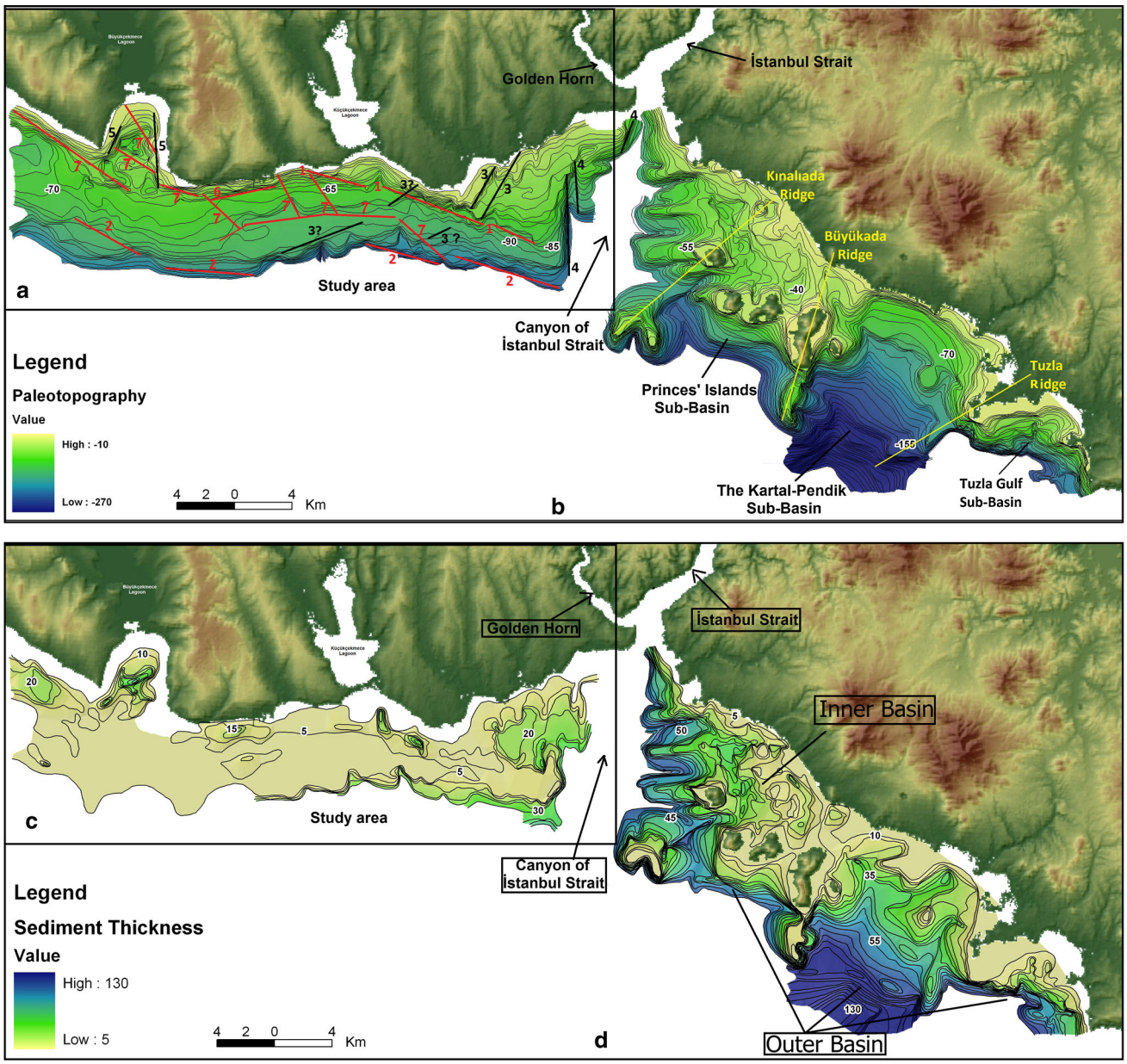

Fig. 16 **a** Paleotopographic map of the basement upper surface layer and lineaments of study area. **b** Paleotopographic map of the basement upper surface layer of the northern and northeastern shelf area. **c** Thickness map of the Plio-Quaternary basin fill along the study area. **d** Thickness map of the Plio-Quaternary basin fill of the northern and northeastern shelf area (modified after Gokceoglu et al. 2009)

As the chaotic reflections of the Lower Unit at the western slope of the canyon are changing to parallel reflections on a seismic profile interrupting the Bosphorus (Gökaşan et al. 2002; Fig. 15a), we consider it to be as a border between the Paleozoic and Oligocene-Upper Miocene-aged units in this area. The Lower Unit is too deep to follow since the top surface of the unit goes under the penetration depth of the energy on the shallow seismic data along the eastern part of the Istanbul Strait Canyon. Nevertheless, the acoustic basement is first seen with a low-angle mature surface morphology in the profiles towards the western slope of the strait. It is also seen that the acoustic basement prominently rises at the western slope of the Istanbul Strait Canyon (Fig. 15a). This unit represented by Oligocene–Upper Miocene-aged units in the area between the Istanbul Strait and Büyükçekmece is located very near the sea bottom in the mentioned area (Figs. 13, 14, 15a). As the top surface of Oligocene–Upper Miocene aged units along Istanbul Peninsula is eroded by Upper Miocene–Pliocene aged mature erosion surface, the upper layer of the offshore continuation of this surface is also affected from this erosion. The shelf of the study area

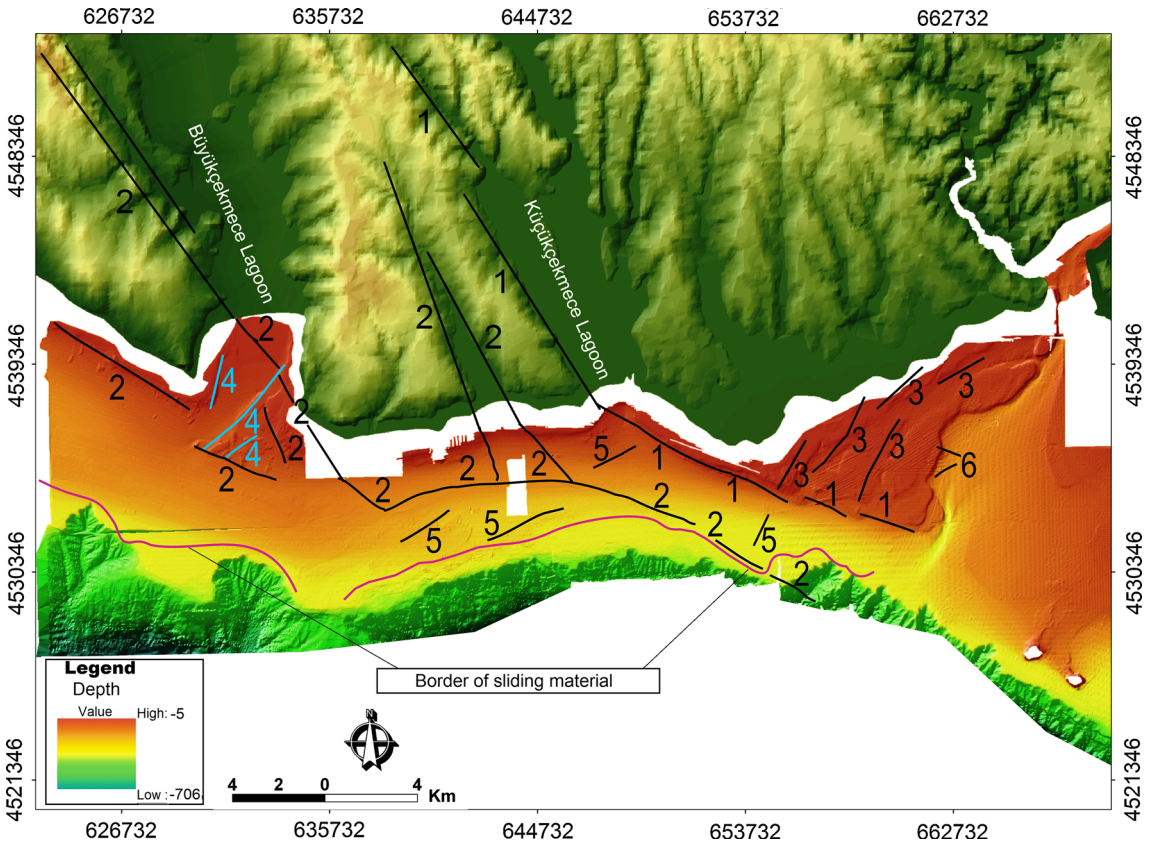

Fig. 17 Map of the young fault observed in the shelf area between the İstanbul Strait and Büyükçekmece Gulf. *Black lines* represent strike-slip faults while *blue lines* represent normal faults. *Red line* represents the border of submarine landslides on the shelf

where the Upper Unit is also relatively very thin is much shallower than the shelf area between the Gulf of Tuzla and the Istanbul Strait. It is shown that two erosional periods must be superimposed. One of them is the Upper Miocene–Pliocene erosional period, and the other is during the Würm glacial period erosional effects caused by the sea level falling on surface in the Pleistocene. Particularly, we consider that the current morphology of the surface which was a land area compared to the Marmara Sea level dropping below −90 m during the latest one of the glacial periods in question and was exposed to transgressive erosion due to sea level rising afterwards must be a ravinement surface emerging as the result of the mentioned transgression. If the effects of the erosional activity in the period are at the eastern part of the study, they are observed on young sediments, not on the Lower Unit.

Since the reflection configuration of the lower unit displays a characteristic deformation, its initial internal parallel reflectors are sighted on the seismic profiles. Indicating an erosional period after deposition, the top of the lower unit is indicated by an angular unconformity. This surface was developed in the course of the Würm glacial age from neighboring areas (Demirbağ et al. 1999; Oktay et al. 2002). Initial deposition under low energy conditions is defined by the parallel reflection configuration of the lower unit. On the other hand, the parts on the seismic profiles called the high deformation zone in the lower unit are less deformed than the lower unit along some narrow zones (Figs. 9a, b, 15a–f). In addition, in these zones, there are some gas charges in the strata of the lower unit on seismic profiles (Fig. 15c, d).

Onshore deposits contain Upper Miocene and older sediments covering onshore and offshore of the study area (Arıç 1955). The Upper Miocene sequence consists of unconsolidated gravel and sand of the base having a variable thickness, and passes through clay-marl-mudstones and muddy limestone towards the top (Arıç 1955). In the light of observed data, the lower unit is part of the submarine extension of the Upper Miocene and older sediments.

Between the upper and the lower units on the truncation surface of the Marmara entrance of İstanbul Strait, a deltaic sequence with an oblique-sigmoidal reflection configuration is observed (Fig. 15a). Oktay et al. (2002) interpreted this sequence as delta deposits, which originated during the Würm glacial period.

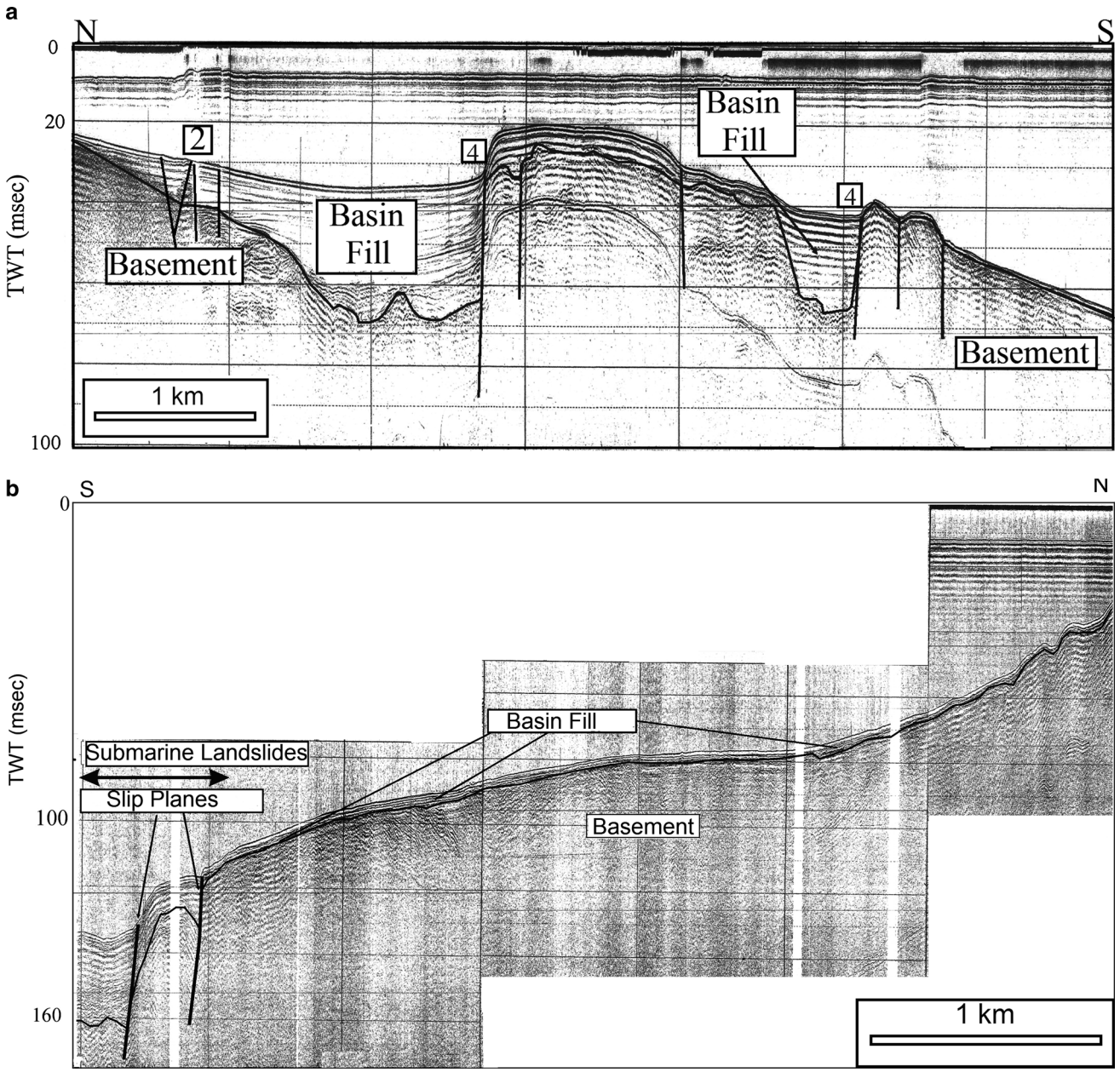

Fig. 18 **a** The group of normal faults n. *4* controlling the eastern slope of the Büyükçekmece Lagoon and the basins formed by this fault group (see Fig. 12 for the site location) and the group of normal faults n. *2* on the Büyükçekmece Gulf. **b** The slip plane formed as the result of the submarine mass movements at the periphery of the shelf and the strike-slip faults on the shelf (see Fig. 12 for the site location). **c** Slip plane formed as the result of submarine mass movements at the periphery of the shelf. The excessive and irregular deformation observed in layers of the acoustic basement and the basin fill in this area suggests that strike-slip fault n. *2* might have an effect on this area in addition to the mass movement (see Fig. 12 for the site location). **d** Fractures of fault groups n. *1* and *3* (see Fig. 12 for the site location)

Upper unit (basin fill) since the internal reflection of this unit end with onlap and downlap on the top of the Oligocene–Upper Miocene acoustic substratum (Fig. 13), this indicates that this unit must be basin fill based on the unit below it, similarly to the shelf area between the gulf of Tuzla and the İstanbul Strait Canyon (Tur 2007). This unit is prominently divided into two sub-units on seismic profiles. The lower one (BF1) has a relatively more chaotic internal reflection formation and is observed in the local channels on the acoustic basement, as well as the periphery of the shelf (Figs. 13, 14). The upper part of the basin deposit (BF2) widely covers the lower deposits (BF1) and the acoustic basement. The top of this sequence, which has a parallel internal reflection formation, crops out at the sea

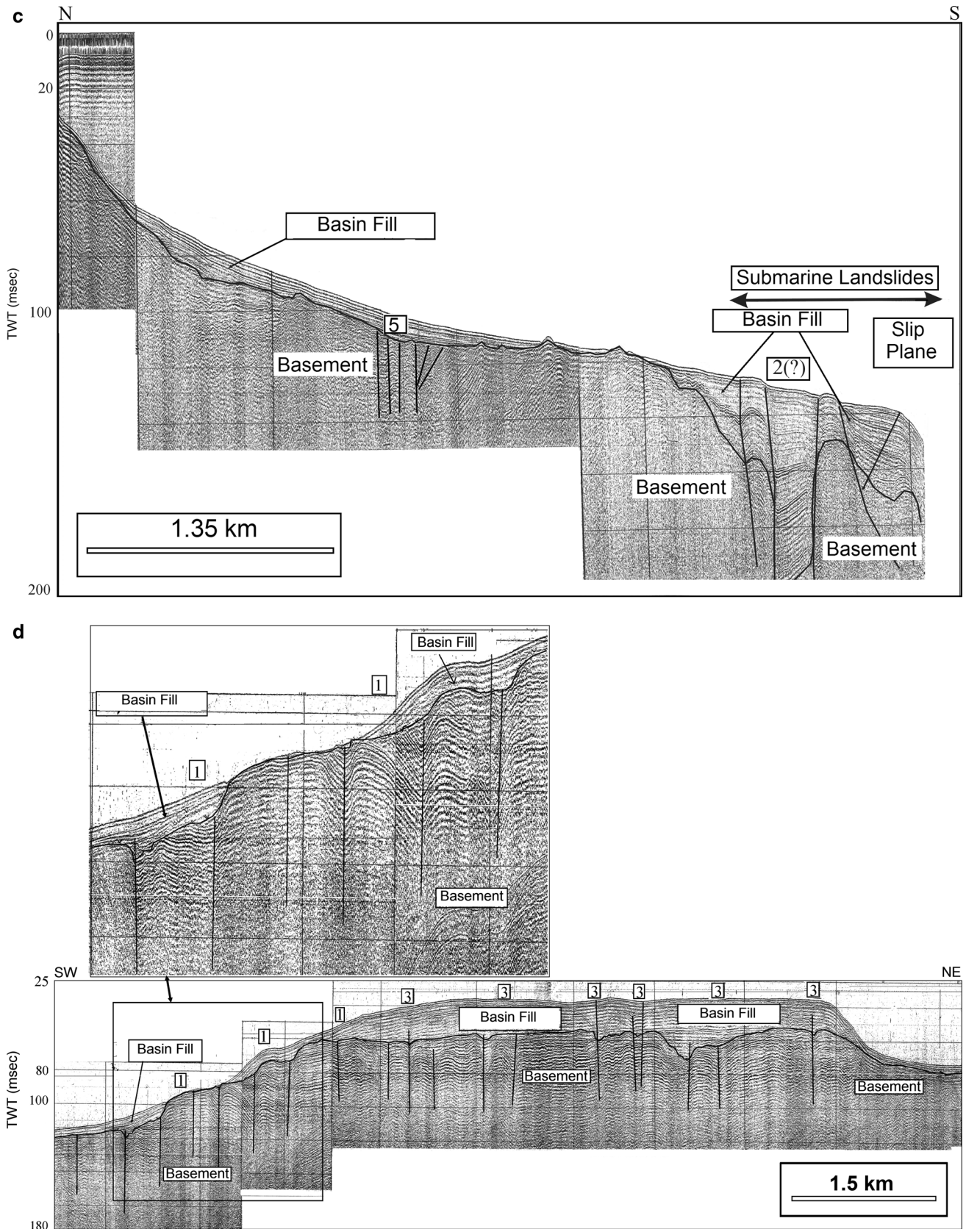

Fig. 18 continued

bottom (Figs. 13, 14). Therefore, we conclude that BF2 must be current sediments settling in this area following the latest glacial period. On the other hand, the underlying hd1 reaches a significant thickness at the periphery of the shelf and reflection formation changes into progressive clinoforms from chaotic or parallel in this area (Fig. 14). Surface layer of this stack is observed to be eroded from the periphery of the shelf (Fig. 14). This data leads to the conclusion that BF2 consists of lowstand deposits settled during the latest glacial period and the coastal clinoforms reflect the beach environment in the said period.

On the northern shelf of the Marmara Sea, the upper unit is disclosed on the truncation surface (Figs. 9a, b, 15a–f). Implying low-energy depositional conditions, this unit is characterized by an internal parallel reflection configuration. In the internal reflector, a truncation surface is not observed. If this upper unit is still actively accreting today, the top of this sequence forms the modern bed. During the Flandrian Transgression (stage of the Holocene epoch (the present geological period), covering the period from around 12,000 years ago, at the end of the last glacial period to the present day), deposition should have been begun. From the seismic profiles, in the highly deformed lower sequence zones and the thickness of the upper unit changing in these zones, the upper unit is deformed together with the truncation surface and sea floor.

Paleo-topography of the top of the acoustic basement, basin fill thickness maps and their geological interpretation

If we consider the top of the Upper Miocene basement unit, this surface has a flat and regular morphology between the Istanbul Strait and Büyükçekmece Gulf in the area of study compared to the area between the Gulf of Tuzla and the İstanbul Strait in the study characterized by basin and ridge systems (Figs. 16a, b). This surface reaches water depths of 50 m with a longshore and lesser than 20° dip angle right at offshore areas of the shore line (Fig. 16a). In a significant part of the shelf, we observed that this surface deepens with low angles from −50 to −100 m towards the periphery of the shelf from the shore. In the periphery of the shelf, it was observed that the inclination and depth values are rapidly increasing and the northern slope of the Marmara Sea is passed on (Fig. 16a). The acoustic basement in this area could be followed up to water depths of 150 m on seismic profiles. A relatively complex morphology is observed on the acoustic basement west of the Bosporus Canyon, at offshore areas of Bakırköy and at the exit of the Büyükçekmece Lagoon in the area between the Bosporus and the Büyükçekmece Lagoon (Fig. 16a). The E–W or NW–SE extension of the shelf turns to the NNE–SSW direction at offshore areas of Bakırköy and some benches are observed on the acoustic basement in this area (Fig. 16a). The most evident one of these benches is observed between the shelf area and the western border of the Bosporus Canyon. Since the shelf represented up to about 50 m depth in this area is deepened rapidly along the western slope of the canyon and drops below the seismic penetration depth, its depth could not be measured along the strait canyon. It has been concluded that the surface layer depth of the acoustic basement in this area must be deeper than −125 m which is the highest value which could be measured on this slope (Fig. 16a). At the exit of the Büyükçekmece Lagoon, it is observed that the surface layer of the acoustic basement has a much more complex morphology and there is a trench consisting of local basins of −70 m depth in this area (Fig. 16a).

Based on paleotopographic interpretation the sedimentary deposits defined as basin fill are significantly thinner compared to those in the area between the İstanbul Strait and the Gulf of Tuzla in the area of study (Fig. 16c, d). The thickness of the basin fills 0–5 m in a major part of the shelf increases locally at the exit of the Küçükçekmece and Büyükçekmece Lagoons (Fig. 16c). In the paleotopography of the acoustic basement, an apparent increase is observed in depth values of the basin fill along a longshore band throughout its slope at offshore areas of the coast and lying parallel with the coast line as well. A significant increase is observed towards the periphery of the shelf in the basin fill (Fig. 16c). Apart from that, it has been concluded that the sediment depth could not be measured and there must be a basin fill thicker than 50 m in this area since the sediment thickness values increase rapidly towards the Bosporus Canyon and the acoustic basement drops below the seismic penetration depth within the canyon (Fig. 16c). Thickness of the basin fill increases rapidly again in the periphery of the shelf. In this area, depth values rapidly reach to 45 m along the northern slope of the Marmara Sea from about 5 m depth on the shelf, and at offshore areas of this area, it is not possible to measure depth values since the seismic penetration depth is exceeded (Fig. 16c).

Based on the top morpohology of the Upper Miocene acoustic basement and the changes in depth values of the basin fill, existence of some tectonic linearities could be inferred (Fig. 16a). Considering the directivity of these lineaments in general, it is seen that the linearities observed in this part of the area of study lie in the NW–SE, N–S, NNE–SSW and ENE–WSW directions (Fig. 16a). The predominant direction of the lineaments is in the E–W trending part of NW–SE. Among the lineaments in the said directions, the one with the greatest continuity is the lineament n. 1 (Fig. 16a). This lineament is identified on the surface younger than the acoustic basement right to offshore of the coast and parallel to the shoreline consists of four lineaments parallel to each other (Fig. 16a). These

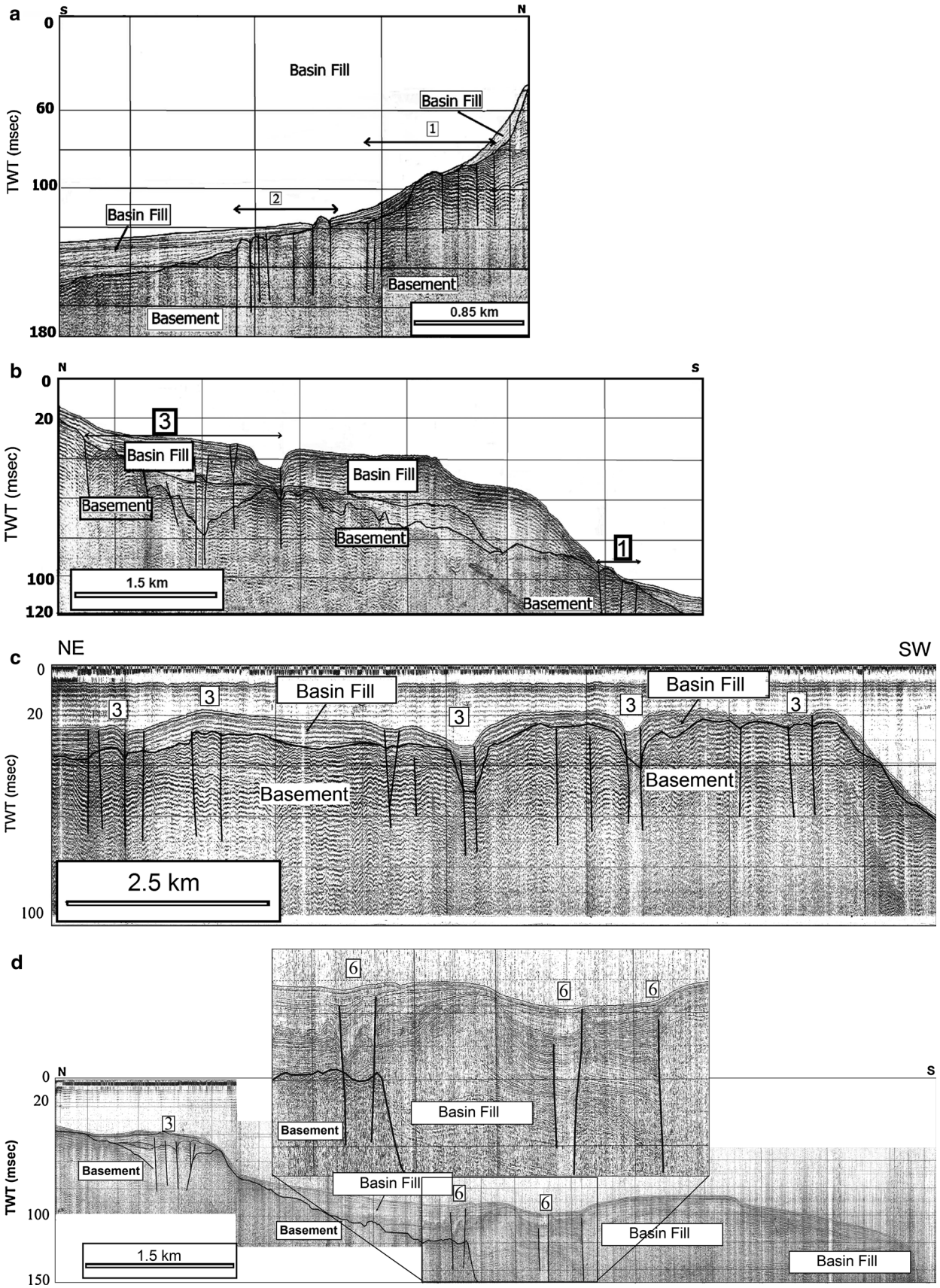
a
S
N
0
60
100
180
TWT (msec)
Basin Fill
Basin Fill
1
2
Basin Fill
Basement
Basement
0.85 km
b
N
S
0
20
100
120
TWT (msec)
3
Basin Fill
Basin Fill
Basement
Basement
1
1.5 km
Basement
c
NE
SW
0
20
100
TWT (msec)
3
3
Basin Fill
3
3
Basin Fill
3
Basement
Basement
2.5 km
d
6
6
6
N
S
0
20
100
150
TWT (msec)
3
Basement
Basement
Basin Fill
Basin Fill
6
6
Basement
Basin Fill
Basin Fill
1.5 km

◀**Fig. 19** **a** Fractures of fault groups n. *1* and *2* (see Fig. 12 for the site location). **b** A fracture from fault groups n. *1* and *2* (see Fig. 12 for the site location). **c** Deformation created by fractures of fault group n. *3* on the sea bottom (see Fig. 12 for the site location). **d** Deformation created by fractures of fault group n. *6* on the sea bottom (see Fig. 12 for the site location)

lineaments have been identified in the sea bottom morphology as well and defined as L2 lineaments (Fig. 11a). The lineament n. 2 at the periphery of the shelf is located on the northern slope of the Marmara Sea and lies in parallel with the lineament n. 1 (Fig. 16a).

The second predominant linearity direction observed in the area of study consists of the lineaments n. 3 and 4 ranging from N–S to NNE–SSW (Fig. 16a). These lineaments have been determined based on the benches observed on the shelf where the shelf turns to the NNE–SSW direction from the E–W direction at offshore areas of Bakırköy and the slope between the shelf and the Istanbul Strait Canyon. It is observed that these lineaments coincide with L1 lineaments observed at the sea bottom (Figs. 11a, 16a). Lineaments in the similar direction lie in parallel with the shore at the exit of the Büyükçekmece Lagoon (lineament n. 5, Fig. 16a). These lineaments coincide with L3 lineament observed in the same area on the sea bottom. The last lineament identified on the acoustic basement in this sector of the study area is the lineament n. 6 represented by the vertical translation at the shore line between the Küçükçekmece and Büyükçekmece Lagoons. This ENE–WSW linearity coincides with L5 lineament observed in the same area on the sea bottom (Figs. 11a, 16a).

Significant differences have been observed in the sediment thickness of both the top and the sea bottom morphology of the acoustic basement and the basin fill between the western part of the study area remaining between the İstanbul Strait Canyon and the Büyükçekmece Lagoon and the eastern part between the Gulf of Tuzla and the İstanbul Strait Canyon. The border of these differences is the İstanbul Strait Canyon which created a significant morphological abnormality with the deep channel structure in this area (Fig. 16b, d).

Considering the paleotopography of the top of the acoustic basement, a significant morphological difference between the western and the eastern part of the study area is evident. While observing the complex morphology consisting of basin and ridge systems of this surface in the eastern part of the study area, it is observed that the western part of the study area is a shelf plain with a depth ranging mostly from −50 to −100 (Fig. 16b, d). Sea bottom morphology of these areas presents quite important differences. The sea bottom in the eastern part of the study area presents a complex morphology due to the elevations represented by the Princes' Islands located in the area while the western part has a morphology of a shelf plain deepening towards the periphery of the shelf mostly with low angles like in surface layer of the acoustic basement. This significant translation observed both in the sea bottom and the surface layer morphology of the acoustic basement along the İstanbul Strait Canyon has the most significant difference in terms of sediment thickness of the basin fill on the acoustic basement in both of these areas (Fig. 16d). There is a basin fill thicker than 100 m within the NNW–SSW sub-basins in the eastern part of the study while the basin fill thickness is below 5 m throughout a major part of the E–W shelf area on the Upper Miocene aged acoustic basement in the western part (Fig. 16d).

All these data demonstrate that the eastern part of the study area became a basin downthrown by normal faults following the erosion during the Upper Miocene–Pliocene, whereas the western part was not affected by formation of sedimentary basins. The basin area included the İstanbul Strait and the western slope of the strait canyon constitutes the border of the basin. In this respect, the İstanbul Strait is located on an important geological border within this evolution. The eastern part of the study area became a depositional area due to down throwing of normal faults and this area was probably filled with a Plio-Quaternary aged thick sediment stack. However, the western part at the west of the strait canyon was an area where there was no or very limited deposition due to its morphology during these periods. The reason must be that the shelf area at the west was evolved mostly as an erosional area during the glacial periods in the Pleistocene and therefore little deposit accumulating in this area was eroded. As a result, the erosion surface observed on the acoustic basement in this area is not only the product of the erosional activity effective in the Upper Miocene–Pliocene period, but a cumulative erosional surface emerging due to the effect of other erosional factors having effect on this area in later periods. In this respect, young erosional effects must enhance this surface by superimposing on the old mature erosion surface. The reason for the upper unit of the deposits on the shelf being located at the west of the İstanbul Strait Canyon consists of the current deposits settling in this area following the latest glacial period and the lower unit existing below it and spreading to a very limited area is the lowstand deposit accumulating during the latest glacial period must be that this area suffered erosion in each glacial period and the deposits accumulating in interglacial periods were eroded. Nevertheless, since the old mature erosion surface deepens and is covered by sediments in the eastern part of the study area deepened as a basin, it must be preserved as a buried residual surface. Traces of erosional effects caused by the low sea level in glacial periods in the Pleistocene and the deposit accumulation caused by the deposition in interglacial periods

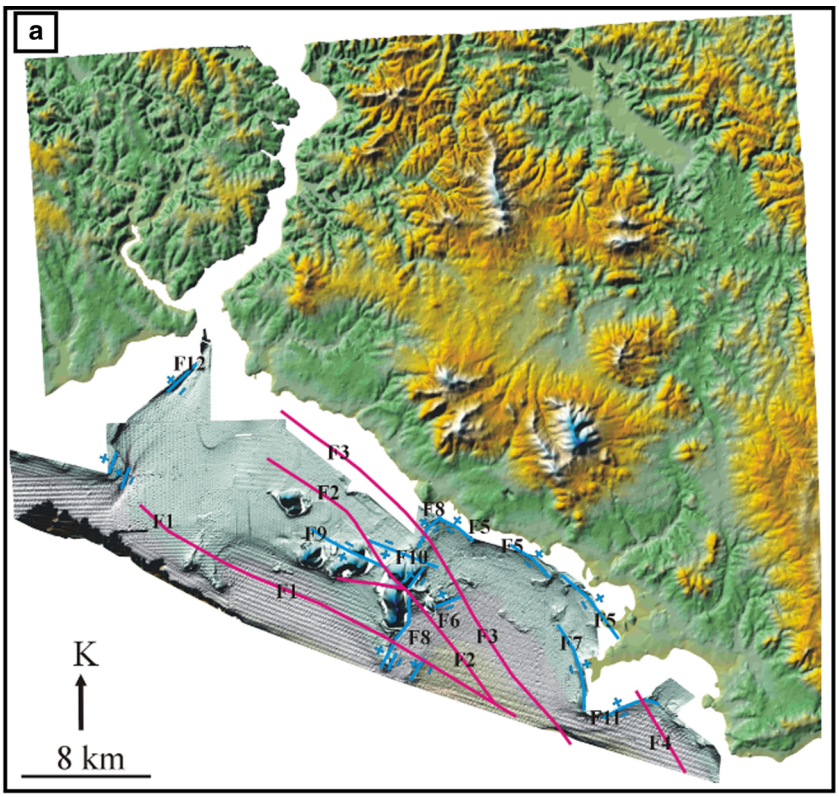
a
F12
F3
F2
F1
F9
F10
F11
F8
F5
F6
F7
F4
K
8 km

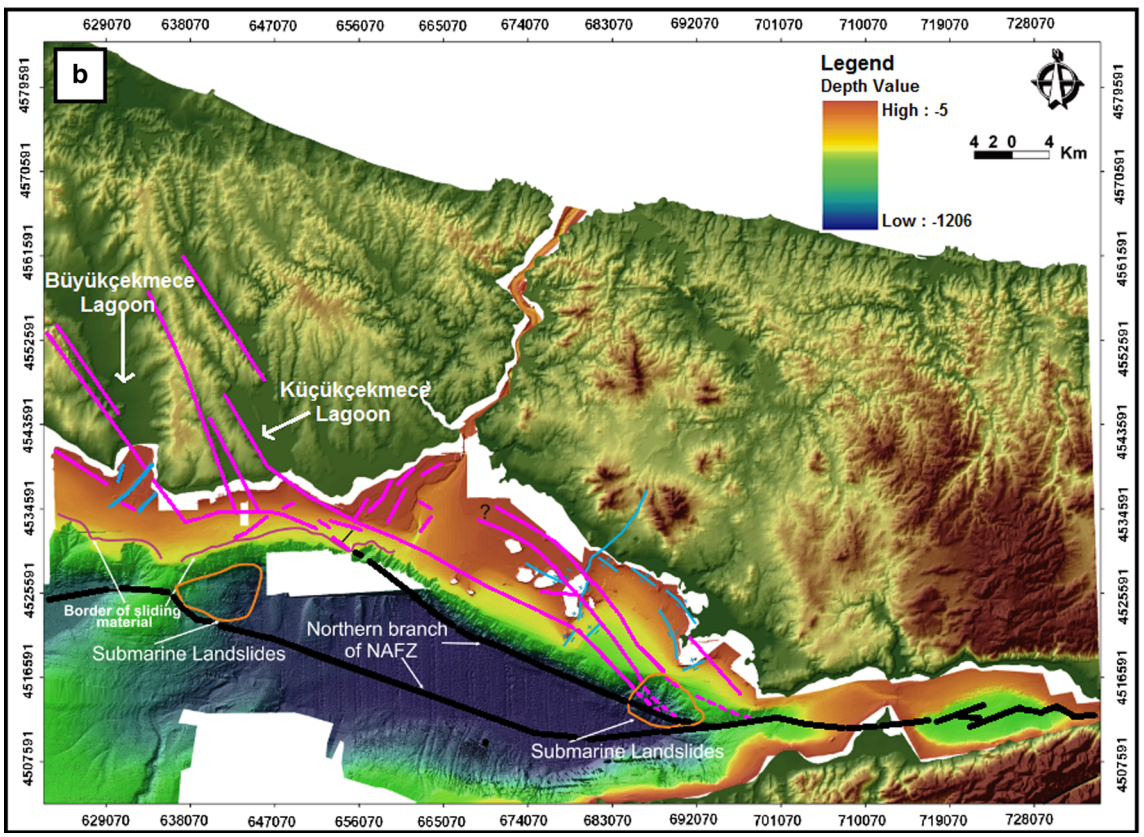
b
629070
638070
647070
656070
665070
674070
683070
692070
701070
710070
719070
728070
4579591
4570591
4561591
4552591
4543591
4534591
4525591
4516591
4507591
Legend
Depth Value
High : -5
Low : -1206
4 2 0 4 Km
Büyükçekmece Lagoon
Küçükçekmece Lagoon
Border of sliding material
Submarine Landslides
Northern branch of NAFZ
Submarine Landslides

◀**Fig. 20** **a** Faults cutting the basin deposits and the sea floor in the İstanbul Strait Canyon-Tuzla Gulf. Faults labeled as *F1–F4* are strike-slip faults. Other faults are normal faults. "+" and "−" indicate footwall and hanging wall of normal faults, respectively (Tur 2007). **b** The faults identified in the study area and the border where the slip plane of the sliding material interrupts the sea bottom at the periphery of the shelf. *Black lines* represent the northern branch of the NAFZ; *red lines* represent the NW–SE and NE–SW strike-slip faults in the study area; *blue lines* represent the NNE–SSW normal faults; and *red* and *orange lines* represent the submarine landslide at slopes

are observed on seismic profiles as many discordant surfaces within the thick basin deposits. Therefore, traces of the erosional effects occurring during the latest glacial period have effects on the young deposits on the uppermost part of the basin fill, not on the acoustic basement as in the western part of the study area. Available data indicates that the area between the Gulf of Tuzla and the western slope of the İstanbul Strait Canyon became a basin within the Plio-Quaternary period. The shelf area at the west of the strait canyon must have continued its evolution as a topographic high with the same characteristics as the land area in its hinterland (Istanbul Peninsula) within this period.

Structural interpretation

The structural interpretation of seismic data has evidenced traces of faults young enough to have an effect on the sea bottom in the shelf area between the İstanbul Strait and Büyükçekmece Gulf (Fig. 17). Among these faults, those represented in blue shown in Fig. 17 are normal faults with a vertical slip component observed in seismic profiles. The black faults have been determined through deformational zones they have created, rather than the vertical shifting of seismic horizons and therefore they are considered to be strike-slip faults.

The normal faults identified in the study area show sudden and sharp vertical shifting of seismic reflectors on the seismic data. Normal faulting in the area between the Gulf of Tuzla and the Istanbul Strait forming the eastern part of the area of study is observed to have vertical effects both on the acoustic basement and the sea bottom. On the other side, the structural elements of the study area between the İstanbul Strait and the Büyükçekmece Gulf constituting the western part have a strike-slip characteristic rather than normal faulting (Fig. 17). In this part of the area of study, the only normal fault observed at the west of the İstanbul Strait is the fault n. F4 controlling the eastern slope of the Büyükçekmece Lagoon (Figs. 15a, 18a). It has been concluded that this fault in the area of study must be NNE–SSW considering the vertical translation it created on the sea bottom and the resultant linearity (Figs. 11a–c, 17). No trace of another apparent and fault-controlled vertical translation on the shelf area between the İstanbul Strait and the Büyükçekmece Gulf.

Nevertheless, vertical translations observed in all profiles with individual sizes along the periphery of the shelf are interpreted as submarine landslides (Fig. 18b, c). On the other hand, it is observed in some seismic profiles that the slip plane of this landslide at the periphery of the shelf is interrupted by strike-slip faults at the periphery of the shelf in some profiles (Fig. 18b, c). The faults in this area show themselves with elevations in the acoustic basement and the basin fill within the sliding mass. Even though such elevations can be considered structures controlled by marine sliding, due to the existence of strike-slip faults, these structures may be tectonically controlled (Gökaşan et al. 2002, 2003).

The second group of faults identified on seismic profiles consists of strike-slip faults. Among these faults, known for the deformations which they have created along certain zones rather than the vertical translations on reflection surfaces, five faults have been identified in the study area (1, 2, 3, 5, 6; Fig. 17). Between these faults, the fault n. 1 is observed to be a single fault zone on the seismic and bathymetric data while other faults are in groups consisting of many fault tracts lying parallel with each other (Fig. 17). The fault group with the greatest continuity is the n. 2. Fault groups n. 3, 5 and 6 consist of relatively shorter faults. Effects of these faults can be traced to the sea bottom on some profiles. One of the most significant faults observed in seismic and bathymetric data is the n. 1 (Figs. 15b, c,18d, 19a, b). Fault n. 1 coincides with the L1 linearity observed on the sea bottom. Therefore, it is observed that the fault borders the high submarine plain at the west of the İstanbul Strait Canyon from the south on seismic profiles (Fig. 18d). Fault n. 1 is observed at the east starting from the west of the İstanbul Strait Canyon (Fig. 18d) and controls the NW–SE linearity (L1) on the sea bottom in this area until the entrance of the Küçükçekmece Lagoon (Fig. 19a, b). This fault represents itself with the folding it created across a narrow zone on layers of the acoustic basement. This vertical slip created by fault n. 1 on the sea bottom shows that this fault must have a vertical component in addition to its strike-slip component. The folding observed in this fault of the acoustic basement on seismic profiles suggests that the vertical movement might be alternatively caused both by a compressional component of the acoustic basement or by inversion processes. We conclude that fault n. 1 must be a young one as the folded acoustic basement rises to and outcrops at the sea bottom on profiles.

Even though the fractures of the fault group n. 2 do not form an apparent vertical slip on the sea bottom and consequently have no apparent linearity, high density of seismic profiles in this area allowed this fault to be well-

observed on profiles and therefore it could be determined that faults composing the group are NW–SE like fault n. 1. Although this group of faults does not form an apparent vertical movement on the sea bottom unlike fault n. 1, it is clearly observed that the effect of this fault on seismic profiles reaches to young deposits and the sea bottom (Figs. 15b–f, 18a, c, 19a). Faults from group n. 2 on seismic profiles are observed as two fractures lying parallel with each other right at the south of the eastern edge of fault n. 1 (Fig. 19a) and at the periphery of the shelf (Figs. 17, 18c, 19a). It is observed that this westward fault lying in the NW–SE direction all the way to offshore areas of Küçükçekmece turns to the south as of this area and gets to the E–W direction approximately (Fig. 17). It is observed that faults from this group lose their effect at the east of the Büyükçekmece Gulf. Faults group n. 2 starts NE–SW trending from Çınarcık Basin in the west of İstanbul Canyon and it extends in front of Küçükçekmece Lagoon E–W oriented. In the west of Büyükçekmece Gulf, faults group n. 2 turns again NW–SE direction and tends to merge with Çatalca fault. It is thought that faults group n. 2 continues to the west and south shelf areas of Büyükçekmece Gulf (Fig. 17). This fault is conformed to L7 lineament in Fig. 16 and to L6 lineament depicted in Fig. 11a.

Fault group n. 3 is clearly observed in bathymetric data due to the effects it created both on seismic profiles and the sea bottom. This group of faults controls the NNE–SSW cavities on the high platform observed on the sea bottom at the west of the İstanbul Strait Canyon (Figs. 11b, c, 15b, 17, 18d, 19b–d). Even though it controls these cavities, since faults caused only deformation along narrow zones instead of creating a vertical slip in parallel with the sea bottom on the deep layers, it indicates that these faults must be strike-slip. Thus, it is thought that narrow trenches appearing across the fault on the sea bottom are likely to be formed as the result of surface effects on the weak zone occurring throughout the fault. Since some of the cavities controlled by the faults in the sea bottom morphology are old valleys joining the İstanbul Strait Canyon while others are located on the marine continuance of the valleys joining the Marmara Sea from Istanbul Peninsula (Fig. 11), its supports the idea of that these cavity areas might be emerged due to the fault-controlled surface flow. Fault n. 3 exists independently from these cavity areas in some parts on the high submarine plain at the west of the İstanbul Strait Canyon (Fig. 19d).

The fault n. 5 is observed in limited areas on the shelf (Figs. 15c, d, 18c). This NNE–SSW fault group is considered to have an original relation with fault n. 3 due to the similarity in the direction of this fault group. Fault group n. 6 consists of two short faults. Since these faults identified based on the deformation observed on young sediments in the İstanbul Strait Canyon (Fig. 19d) are observed in a limited area on seismic profiles, it suggests that these faults might be secondary structures formed due to the deformation created in the area by more predominant structures such as fault n. 1.

The lineament L6 (Fig. 11) seen in the land topographic map were interpreted as faults by Ergintav et al. 2011. Because of similarity between them and faults in the shelf area, faults in the sea and land are correlated (Fig. 17).

After morphological, bathymetric, seismic evaluations and interpretations, faults group no. 1, 2, 3, 5 and 6 are strike-slip faults while fault group no. 4 is normal fault as seen in Fig. 20b.

Discussion

While between the Büyükçekmece Gulf and the İstanbul Strait Canyon from the northern shelf of the Marmara Sea lies in the E–W direction approximately, it turns into the NNE-SSW direction in the part between the western slope and the shore line of the Bosporus canyon. The İstanbul Strait Canyon segregates the area of study and the part at the east of the shelf from each other.

The geological interpretation of seismic and bathymetric data indicates that the top of the Upper Miocene acoustic basement has an almost horizontal and highly uniform morphology along its E–W part. The horizontal plan formed by the top of the acoustic basement across the shelf is interrupted by slopes at the shore line and the periphery of the shelf. The one at the shore line of these slopes causes the Upper Miocene-aged acoustic basement to come down from 0 m to −50 m. The top of the acoustic basement forms a horizontal plan ranging from −50 to −100 m along the shelf plain and extends to the periphery of the shelf with low angles. Inclination and depth of the E–W part of the shelf increase suddenly at the periphery of the shelf and the shelf area turns into the northern slope of the Marmara Sea. In the NNE–SSW part of the shelf which remains between the İstanbul Strait Canyon and the shore, a more complex morphology is observed in the top of the acoustic basement. This complexity is demonstrated by itself with NNE–SSW benches observed on the shelf and the western slope of the İstanbul Strait Canyon in the same direction. Another complex area seen in the morphology of the top of the acoustic basement is a local basin at the exit of the Büyükçekmece Lagoon.

Some NW–SE and NNE–SSW linearities observed in surface layer of the acoustic basement and on the sea bottom are determined to be fault-originated as the result of their comparison with seismic profiles. In seismic profiles, we conclude that sediment offset by these faults is young deposits considered to be settled due to the phenomena during and after the latest glacial period. Those lying in the

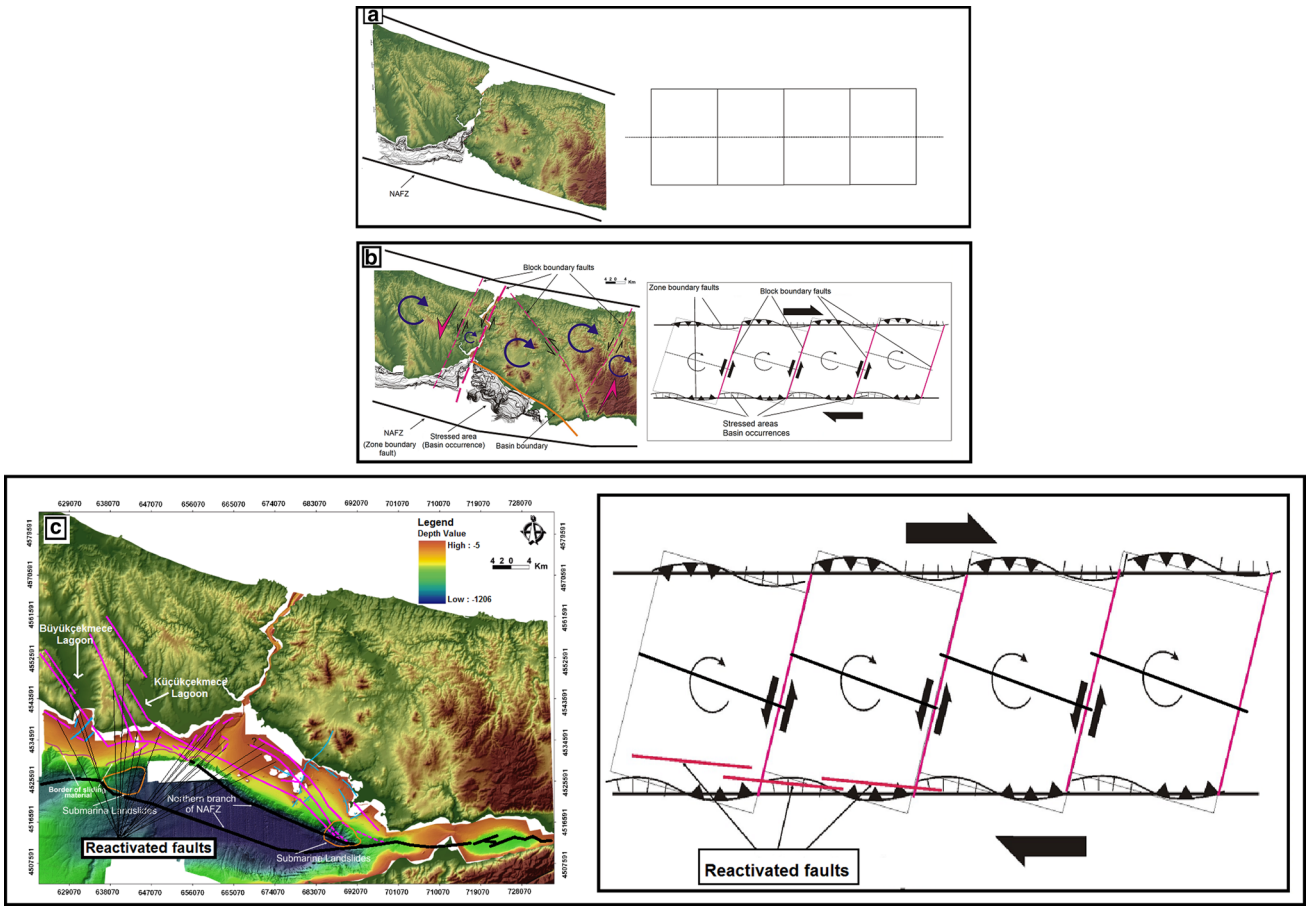

Fig. 21 Tectonic evolution model of the study area

NNE–SSW direction of these faults are interpreted as normal faults due to the vertical translations they created on the sea bottom and the units below it. Of these faults, it is observed that particularly the fault controlling the western slope of the Bosporus has created a vertical slip at highly significant levels and borders the thick sediment stack observed in the strait canyon. West of this fault, sediment thickness does not exceed 5 m in a major part of the shelf area. Therefore, it is considered that the fault at the western slope of the strait canyon must be a border in terms of development of basins identified in the part between the Gulf of Tuzla and the İstanbul Strait Canyon constituting the eastern part of the study. Other normal faults in this area control the exit of the Büyükçekmece Lagoon.

In the study area the faults interpreted as strike-slip faults are generally NW–SE oriented. These faults must also have a vertical component due to benching they created both in the acoustic basement topography and the sea bottom. Of these, the fault following the shore line from offshore areas of the Küçükçekmece Lagoon to the İstanbul Strait Canyon is one of the faults with the greatest continuity in the area of study.

Comparison of the faults in the northern shelf of the Marmara Sea between the Büyükçekmece Lagoon and the Gulf of Tuzla

Two group of faults have been identified which are different from each other in terms of their extension and slips in the study area (Fig. 20a, b). The first one of these fault groups limits mostly the basins identified in the study area. These faults must be normal or oblique faults with a high vertical component due to the vertical slip they created on the reflection surfaces of the acoustic basement observed in seismic profiles and the basin fill on it. These faults with the extensions lying in directions ranging from N–S to NNE–SSW in the study area have been encountered often on the borders of sub-basins in the same direction and ridges in between at the eastern part of the study area (Fig. 20a, b). The faults in this group are shorter but more in quantity than those in the second group. The change in

the geometry or frequency of the faults is primarily related with areas where the basins are located in and also related to the geometry of these basins. For this reason, we conclude that the faults of this group compose the basin-ridge system in this area. The faults in this group are mostly observed in the area between the Gulf of Tuzla and the İstanbul Strait Canyon which constitutes the eastern part. The area where NNE–SSW normal faults are mostly observed ends at the western slope of the İstanbul Strait Canyon (Fig. 20a, b). In the western part of the study area, the faults lying in this direction and developing under the domination of normal fault component are seen only at the exit of the Büyükçekmece Lagoon. Since faults in this group interrupt the erosion surface matured in the Upper Miocene–Pliocene period and compose the basin-ridge system developed at the eastern part of the study area, they must have been activated in the Plio-Quaternary period. These faults' bordering or interrupting in patches young deposits of the basin fill indicates that they maintained their activity up to the advanced stages of basin formation. However, because of the sea level falling during the latest glacial period, since the faults covered by the basin fill are re-revealed due to the erosional activities, possible effects of these faults on the sea bottom could not be fully understood. Likely, faults at the western slope of the İstanbul Strait Canyon can be retreated due to external factors like their conjugates at the east based on the doubt of a possible submarine landslide in this area. Therefore, current activity of faults in this group could not be fully understood.

Among the faults identified in the study area, those in the second group do not present an apparent vertical slip on the acoustic basement and the layers of the deposits on it or have a low-level vertical slip component. Based on these characteristics of them, it is considered that those NW–SE faults must be strike-slip faults or oblique faults with a dominant strike-slip component. Geometry or location of the faults in this group is independent from geometry or distribution of the basins unlike those in the first group. The basin-ridge system with an extension in the same direction as the faults in this group which has a different direction with their NW–SE extension compared to the NNE-SSW basin-ridge system identified in the study area are internal and external basins which are less apparent in morphological terms (Figs. 16, 20a). It is observed that the faults in this group have continuity in longer distances even though their effect on the surface layer morphology of the acoustic basement is less. Especially, fault n. 1 clearly observed at the western part of the study begins at the periphery of the shelf identified at offshore areas of Cape Tuzla, covers the shelf in the NW–SE direction by passing from the south of Büyükada, and then reaches to the north of Sivriada and Yassıada. Fault n. 1 at the western part of the study area is considered to be the fault n. 1's extension at the west. In this case, Fault n. 1 continues in the same direction in the western part of the study as well and reaches to the Küçükçekmece Lagoon (Fig. 20b). Similarly, it seems possible that the faults in the same direction and with the same characteristics at both areas of the study are conjugates and were developed as the product of the same tectonic activity even though they do not unite (Fig. 20b).

Tectonic evolution of the northern shelf of the Marmara Sea between the Gulf of Tuzla and the Büyükçekmece lagoon

To describe the tectonic evolution of the study area, it would be proper to use the models created to explain the formation of the İstanbul Strait right in the northern continuation of this area in addition to the data obtained from the northern shelf of the Marmara Sea. Sub-basins between the NNE-SSW oriented ridges observed along the external basin in the study area show similarities with general characteristics of the İstanbul Strait in terms of both their extensions and existence of the young thick sediment stack accumulated in them (Yılmaz and Sakınç 1990; Yıldırım et al. 1992; Gökaşan et al. 1997). Geological studies on the Istanbul Strait (Gökaşan et al. 1997) have evidenced that the strait started to evolve as a river valley and in the later stages it became a NNE–SSW narrow basin and in the last stage this channel was translated by being interrupted by the faults formed as the result of the new shearing regime it entered with the effect of the NAFZ and thus gained its current shape. Oktay et al. (2002) assert that the aforementioned stages of the strait evolution can be explained through the model of rotations in the blocks between the fault zones analytically modeled by Dibblee (1977) and subsequent formation of secondary block border faults. The authors assert in this model that the İstanbul-Kocaeli high field between the NAFZ at the south and the fault lying parallel with the Black Sea coast suggested by Demirbağ et al. (1999) at the north were forced to rotate clockwise due to movement of these faults and thus it performed this rotation by being divided into smaller blocks. It is asserted that, for such rotation of the blocks, one of the NNE–SSW left-lateral strike-slip faults developed between them caused the deformation creating the current İstanbul Strait (Oktay et al. 2002). Based on the theory that there must be compression areas due to block rotations and local basin developments due to stress areas along the NAFZ forming the zone border faults bordering the rotating block from the south and the north and along the fault at the Black Sea coast, the authors also assert that basins and compression areas must have developed at the eastern half of the northern shelf of the Marmara Sea and at the western edge

of the southern shelf of the Black Sea (Oktay et al. 2002). Based on the model suggested by Oktay et al. (2002), we consider that it is possible to explain the origin of the basin formed in the area between the Gulf of Tuzla and the İstanbul Strait Canyon forming the eastern part of the study area and why this basin suddenly disappears as of the west of the Strait Canyon and accordingly to create a tectonic evolution model for the study area.

In the beginning stage of this model, the İstanbul–Kocaeli high field was a narrow high field located between the Black Sea whose formation happened during the Jurassic period (Finetti et al. 1988) and the Marmara Sea which became a basin in the Upper Miocene (Sakınç et al. 1999; Gökaşan et al. 2003) (Fig. 21a). In this stage, the İstanbul Strait was only a river valley yet. When the NAFZ was activated as a shearing zone and the Marmara Sea in the Plio-Quaternary period (Gökaşan et al. 2003), the Istanbul–Kocaeli elevation started to be deformed between this fault and the fault located at the Black Sea coast. During this deformation the İstanbul-Kocaeli high started to rotate clockwise between the zone border faults (the NAFZ and the fault at the Black Sea coast) and during this rotation, the NNE-SSW oriented left-lateral faults were developed and caused the Istanbul–Kocaeli Elevation to divide into smaller blocks (Fig. 21b). Of these faults, the one in the area where the İstanbul Strait is located deepened faster than the others possibly with the effect of the old strait stream existing in this area and caused the NNE–SSW primary channel to form in the formation of the strait. In the meantime, small blocks belonging to the Istanbul–Kocaeli high rotating clockwise led to formation of stress and compression areas along the left-lateral translations located at both sides of the elevation and consequently the zone border faults (Fig. 21b). Borders of these stress and compression areas at their engagement areas along the zone border faults were controlled by the block border faults. A stress and consequently a triangle-shaped basin emerged in the area between the Gulf of Tuzla and the İstanbul Strait Canyon which is the area located at the east of the fault along the İstanbul Strait valley which is one of the block border faults of this system on the shelf of the Marmara Sea. Since in the part of the study area standing between the İstanbul Strait Canyon at the west of the fault and the Büyükçekmece Lagoon, the block rotation created a compression in the zone border fault, there was no basin formation in that area. Instead, presumably, compression structures observed in Upper Miocene aged units were developed in that area (Fig. 21b). According to this model suggested, the NNE–SSW faults observed in the study area and bordering the İstanbul Strait Canyon with sub-basins must be block border faults. The most important of these faults is the fault existing in the İstanbul Strait Canyon and this fault segregates the eastern (between the Gulf of Tuzla and the İstanbul Strait) and the western (the İstanbul Strait and the Büyükçekmece Lagoon) parts of the study area and consequently causes the development of the basin at the east and the high field at the west on surface layer of the acoustic basement.

The origin of the NW–SE faults observed in the study area is more complex. These faults might be the NW–SE conjugate block border faults expected to develop with the NNE–SSE block border faults in the block rotation model described above. In this case, the NW–SE faults and NNE–SSW faults are required to develop simultaneously. However, since the NW–SE oriented faults are younger than the NNE–SSW oriented ones and these faults disharmoniously interrupt the structures formed as the result of block rotations, it suggest that they might be formed by the effect of tectonism which developed later. This approach also conforms with the idea suggested by Gökaşan et al. (1997) that the NNE–SSW strait graben was interrupted by the strike-slip faults which developed later and thus the strait gained its current shape.

This interpretation asserting that the NW–SE strike-slip faults identified in the study area were formed by reactivation of some of the faults in Istanbul and Kocaeli Peninsulas as the result of the effect of the NAFZ's new fracture occurring in the Marmara Sea is considered more consistent with the data obtained from this study. Accordingly, the area broken down by the block border faults in the NNE–SSW direction and turning into Istanbul and Kocaeli Peninsulas were broken down in the NW–SE direction this time possibly as the result of reactivation of the old faults as syntectonic structures due to the effect created by the NAFZ's new fracture in this area (Fig. 21c).

Since this tectonism occurring right at the east of the NAFZ has a nature of a secondary structure considering the tectonic activity caused by the NAFZ, there must be relatively much less stress accumulation in these secondary faults compared to the NAFZ. For this reason, faults identified in the study are must be working relatively very slow and as a result, either causing only microseismic activity or earthquake generation periods at very long intervals. Nevertheless, two middle sized earthquakes ($M_W = 4.2$ and $MW = 4.4$) occurring in the study area following the earthquake on 17th August 1999 (Pınar et al. 2003) show that the tectonic activity in this area has the potential to generate earthquakes.

Conclusions

The seismic and multibeam bathymetric research conducted in the area between the Istanbul Strait and the Büyükçekmece Lagoon in the northern shelf of the Marmara Sea has allowed us to reach the following conclusions.

The eastern part between the Gulf of Tuzla and the Bosporus Canyon, and the part between the Bosporus Canyon and the Büyükçekmece Lagoon present different geological and morphological characteristics.

The bathymetry indicates that the sea bottom morphology at the east of the study area has a more complicated structure compared to the study area and there is an internal basin formed on the shelf, in this area between the Princes' Islands and the mainland and for the other area, an external basin on the shelf (Tur 2007). On the other hand, the sea bottom morphology in the study area indicates the existence of a plain deepening seaward with an almost horizontal angle.

The seismic interpretation allowed us to identify two seismo-stratigraphic units. The lower one is separated from the overlying units by a high-amplitude reflector. This unit has chaotic internal reflection in general at the east of the study area while presenting an internal reflection formation changing from chaotic to parallel at the western part. Since these units get close to the sea bottom rising landwards this suggests that they are the marine continuation of the Paleozoic and Upper Miocene units widely cropping out on land. In this case, the lower unit identified in seismic profiles at the east of the study area must be the submarine extension of the Paleozoic units, while the lower one is the Upper Miocene unit (Tur 2007). The high-amplitude reflector forming these units must be an erosional surface developed during the Upper Miocene-Pliocene. The upper unit existing on the acoustic basement whose parallel internal reflections end with onlap and downlap is defined as Plio-Quaternary basin fill.

The morphological interpretation of paleotopography of the top of the acoustic basement identified in the seismic profiles has supported the morphological differences among the study area and the shelf to the east. Here we observed that the top of the acoustic basement is characterized by a basin with sediment fill of 250 m in the east of the study area. The westernmost of these NNE–SSE basins is the Bosporus Canyon. In the study area located at the west of the strait canyon, the paleotopography of surface layer of the acoustic basement forms an almost horizontal shallow plain ranging from −50 to −100 m.

The basin fill thickness identified in seismic profiles also shows a significant difference in eastern and western parts of the study area. A basin fill with a thickness exceeding 130 m is observed within the NNE–SSW basins at the eastern part of the study area while in the western part, these thickness values are determined to suddenly drop below 5 m along the shelf as of the west of the Bosporus Canyon.

The first one of these fault groups in the study area is the NNE–SSW oblique faults with high vertical slip component. These faults are limited by the NNE–SSW deep basins. These faults observed mainly at the eastern part of the study area control the western slope of the Bosporus Canyon and effectiveness of these faults decreases at the west of this slope.

The sea bottom morphology in the study area, the morphology of the top of the acoustic basement, the basin fill thickness and the distribution of the NNE–SSW trending faults bordering the basins on the acoustic basement show that the eastern part of the study area between the Gulf of Tuzla and the Bosporus Canyon and the western part between the Bosporus Canyon and the Büyükçekmece Lagoon have very different structures from each other. The Bosporus Canyon constitutes the border of this significant difference.

The idea suggested by Oktay et al. (2002) for formation of the Bosporus in previous studies asserting that one of the block border faults developed due to the rotations occurring in the areas between the zone border faults must have an important role in formation of the Bosporus has been used to explain this translation in the eastern and western parts of this study area.

According to this model, the Bosporus has emerged due to the clockwise rotations occurring in the Istanbul–Kocaeli high field between the NAFZ and the fault at the Black Sea coast. Based on this system, left-lateral faults must have emerged between clockwise-rotating blocks and one of these faults must have formed the Bosporus. Based on this model, the entire Bosporus including the canyon on the shelf is a block border fault. Compression and stress areas have emerged between the blocks rotated clockwise by the block border faults and the zone border faults due to block rotations.

In the suggested model, a basin must be formed to the east of this fault and a compression area at the west due to block rotations. In this case, the basin-ridge system formed at the eastern part of the study area between the Gulf of Tuzla and the Bosporus Canyon and suddenly ending at the western slope of the strait canyon must be a product of the stress caused by these block rotations. Thus, the question why the NNE–SSW faults lost their effect at the west of the Bosporus Canyon will be answered. The area between the Bosporus Canyon and the Büyükçekmece Lagoon forming the western part of the study area was not affected from this formation of basin since it is located at the west of the block border fault. Compressions that must occur in this area instead of it is represented by common folds observed in the Upper Miocene units in this area.

The second group of faults identified in the study area consists of NW–SE oblique faults with a dominant strike-slip component. It is observed that these faults interrupt the basins instead of bordering them and create the linearities in the same direction in the sea bottom. As the result of the analysis of the relation between these two fault groups, it

has been concluded that the NW–SE faults were activated after the NNE–SSW faults. In addition, as the result of the comparison of these NW–SE faults with the NAFZ, it is possible that this fault group has a relation with the NAFZ. Therefore, it is considered that these faults might be the faults reactivated in the area due to the stress caused by the NAFZ.

It is suggested after morphological, bathymetric, seismic evaluations and interpretations that faults group no. 1, 2, 3, 5 and 6 are strike-slip faults whereas fault group no. 4 is a normal fault. All the faults identified in the study area are secondary faults, as the NAFZ, which is the main fault zone in the Marmara Sea, passes at the south of the study area. In this case, these faults must have a low seismic activity level. Therefore, faults identified in the study area can be considered to possibly create the micro-earthquakes recorded in the area.

Acknowledgments The authors would like to thank the editor and three anonymous reviwers for their suggestions and valuable comments that greatly improved the manuscript. We would like to also thank the Turkish Navy, the Department of Navigation, Hydrography and Oceanography, and the personnel of the R/V T.C.G Cubuklu and Cesme for their enthusiasm and care during the bathymetric data collection. This study was supported by grants from the Istanbul University, Scientific Research Projects Cooordination Unit, project numbers 5783 and 15676.

References

Akarvardar S, Feigl KL, Ergintav S (2009) Ground deformation in an area later damaged by an earthquake: monitoring the Avcilar district of Istanbul, Turkey, by satellite radar interferometry 1992–1999. Geophys. J. Int. 178:976–988

Aksu AE, Calon TJ, Hicott RN (2000) Anatomy of the North Anatolian Fault Zone in the Marmara Sea, Western Turkey: extensional basins above a continental transform. GSA Today 10(6):3–7

Alavi SN, Okyar M, Timur K (1989) Late Quaternary sedimentation in the Strait of Bosphorus: high resolution seismic profiling. Mar. Geol. 89:185–205

Algan O, Yalçın MN, Özdoğan M, Yılmaz Y, Sarı E, Kırcı-Elmas E, Yılmaz İ, Bulkan Ö, Ongan D, Gazioğlu C, Nazik A, Polat MA, Meriç E (2011) Holocene coastal change in the ancient harbor of Yenikapı–İstanbul and its impact on cultural history. Quat Res 76(2011):30–45

Arıç C (1955) Haliç ve Küçükçekmece Gölü bölgesinin jeolojisi (Geology of Golden Horn and Küçükçekmece Lake regions, in Turkish). Ph.D. Thesis, İstanbul Technical University

Armijo R, Meyer B, Navarro S, King G, Barka A (2002) Asymmetric slip partitioning in the Sea of Marmara pull-apart: a clue to propagation process of the North Anatolian Fault. Terra Nova 14:80–86

Armijo R et al (2005) Submarine fault scarps in the Sea of Marmara pull-apart (North Anatolian Fault): implications for seismic hazard in Istanbul. Geochem. Geophys. Geosyst. 6:Q06009. doi:10.1029/2004GC000896

Barka A, Hanckok PL (1985) Tectonic interpretation of enigmatic structures in the North Anatolian fault zone. J. Struct. Geol. 5:217–220

Barka AA, Kadinsky-Cade K (1988) Strike-slip fault geometry in Turkey and its influence on earthquake activity. Tectonics 7(3):663–684

Chaput E (1936) Voyages d'études géologiques et géomorphogénétiques en Turquie. Mém. Institut Francais d'Archéologie de İstanbul 2

Cvijic J (1908) Grundlinien der Geographie und Geologie von Mazedonien und Altserbien. Petermans Mitteilungen Erganzungsheft I(162), Gotha

Demirbağ E, Gökaşan E, Oktay FY, Şimşek M, Yüce H (1999) The last sea level changes in the Black Sea: evidence from the seismic data. Mar. Geol. 157:249–265

Demirbağ E, Rangin C, Le Pichon X, Şengör AMC (2003) Investigation of the tectonics of the Main Marmara Fault by means of deep towed seismic data. Tectonophysics 361:1–19

Dibblee TW (1977) Strike-slip tectonics of the San Andreas fault and its role in Cenozoic Basin evolvement. In: Nilsen TH (ed) Late Mesozoic and cenozoic sedimentation and tectonics in California, San Joaquin Geological Society Short Course, Bakersfield, California, pp 26–38

Dogan U, Oz D, Ergintav S (2013) Kinematics of landslide estimated by repeated GPS measurements in the Avcilar region of Istanbul, Turkey. Stud. Geophys. Geod. 57:217–232. doi:10.1007/s11200-012-1147-x

Duman TY et al (2004) Istanbul Metropol'u Batısındaki (Kucukcekmece-Silivri-Catalca Yoresi) Kentsel Gelisme Alanlarının Yerbilim Verileri. Maden Tetkik ve Arama Genel Mudurlugu (MTA) Ozel Yayın Serisi-3, Ankara

Ergintav S, Demirbag E, Ediger V, Saatcılar R, Inan S, Cankurtaranlar A, Dikbas A, Bas M (2011) Structural framework of onshore and offshore Avcılar, Istanbul under the influence of the North Anatolian fault. Geophys. J. Int. 185:93–105

Erinç S (2000) Jeomorfoloji I (Fifty edition, modified by Ertek A, Güneysu C). Der Press, İstanbul

Finetti I, Bricchi G, Del Ben A, Pipan M, Xuan Z (1988) Geophysical study of the Black Sea. Bollettino di Geofisika Teorica ed Applicata XXX(117–118):197–324

Gazioğlu C, Gökaşan E, Algan O, Yücel ZY, Tok B, Doğan E (2002) Morphologic features of the Marmara Sea from multibeam data. Mar. Geol. 190(1–2):333–356

Gökaşan E (2000) VI. Bölüm: Marmara Denizi'nin jeolojik özellikleri, Marmara Denizi'nin Jeolojik Oşinografisi (Editörler: E. Doğan ve A. Kurter), 177–393, ISBN 975-404-579-8, Umur Matbaacılık

Gökaşan E, Demirbağ E, Oktay FY, Ecevitoğlu B, Şimşek M, Yüce H (1997) On the origin of the Bosphorus. Mar. Geol. 140:183–197

Gökaşan E, Alpar B, Gazioğlu C, Yücel ZY, Tok B, Doğan E, Güneysu C (2001) Active tectonics of the Izmit Gulf (NE Marmara Sea): from high resolution seismic and multibeam bathymetry data. Mar. Geol. 175(1–4):271–294

Gökaşan E, Gazioğlu C, Alpar B, Yücel ZY, Ersoy S, Gündoğdu O, Yaltırak C, Tok B (2002) Evidences of NW extension of the North Anatolian Fault Zone in the Marmara Sea; a new approach to the 17 August 1999 Marmara Sea earthquake. Geo-Mar. Lett. 21:183–199

Gökaşan E, Ustaömer T, Gazioğlu C, Yücel ZY, Öztürk K, Tur H, Ecevitoğlu B, Tok B (2003) Morpho-tectonic evolution of the Marmara Sea inferred from multibeam bathymetric and seismic data. Geo-Mar. Lett. 23(1):19–33

Gökaşan E, Algan O, Tur H, Ecevitoğlu B, Türker A, Caner H, Ertek A, Kırcı E, Sarı E, Görüm T, Erginal E, Direk Ş, Birkan H, Tok B, Şimşek M (2004) Multibeam batimetrik, sismik ve sedimentolojik verilerle, olası genç fayların İstanbul Boğazı boyunca izlenmesi ve Geç Kuvaterner (Holosen) dönemi boğaz evrimi ile son Akdeniz-Karadeniz bağlantısının incelenmesi, İ.Ü. Araştırma Projeleri Yürütücü Sekreterliği (Yayınlanmamış)

Gökaşan E, Tur H, Ecevitoğlu B, Görüm T, Türker A, Tok B, Çağlak F, Birkan H, Şimşek M (2005) Evidence and implications of massive erosion along the Strait of İstanbul (Bosphorus). Geo-Mar. Lett. 25:324–342

Gökaşan E, Tur H, Ecevitoğlu B, Görüm T, Türker A, Tok B, Birkan H (2006) İstanbul Boğazı deniz tabanı morfolojisini denetleyen etkenler: Son buzul dönemi sonrası aşınma izlerinin kanıtları. Yerbilimleri 27(3):143–161

Gokceoglu C, Tunusluoglu MC, Gorum T, Tur H, Gokasan E, Tekkeli AB, Batuk F, Alp H (2009) Description of dynamics of the Tuzla Landslide and its implications for further landslides in the northern slope and shelf of the Cinarcik Basin (Marmara Sea, Turkey). Eng. Geol. 106:133–153

Gürbüz C, Aktar M, Eyidoğan H, Cisternas A, Haessler H, Barka A, Ergin M, Türkelli N, Polat O, Ucer SB, Kuleli S, Bariş S, Kaypak B, Bekler T, Zor E, Biçmen F, Yörük A (2000) The seismotectonics of the Marmara Region (Turkey): results from a microseismic experiment. Tectonophysics 316:1–17

İmren C, Le Pichon X, Rangin C, Demirbağ E, Ecevitoğlu B, Görür N (2001) The North Anatolian Fault within the Sea of Marmara: a new evaluation based on multichannel seismic and multibeam data. Earth Planet Sci Lett 186:143–158

Ketin İ (1948) Uber die tektonisch-mechanischenFolgerungenaus der grossenanatolischenErdbeben des letztenDezenniums. Geol-Rundsch 36:77–83

Koral H and Şen Ş (1994) Evidence of transtensional regime in the Tertiary sediments of İstanbul–Çekmece regions. First Turkish International Symposium on Deformations, İstanbul. Proceedings, pp 680–692

Kuşçu Y, Okamura M, Matsuoka H, Awata Y (2002) Active faults in the Gulf of Izmit on the North Anatolian Fault, NW Turkey: a high resolution shallow seismic study. Mar. Geol. 190(1–2):421–433

Le Pichon X, Şengör AMC, Demirbağ E, Rangin C, İmren C, Armijo R, Görür N, Cağatay N, Mercier de Lepinay B, Meyer B, Saatcılar R, Tok B (2001) The active main Marmara Fault. Earth Planet Sci Lett 192:595–616

McClusky S, Balassanian S, Barka A et al (2000) Global positioning system constraints on plate kinematics and dynamics in the Eastern Mediterranean and Caucasus. J. Geophys. Res. 105:5695–5719

Meriç E, Oktay FY, Sakınç M, Gülen D, İnal A (1991a) Ayamama (Bakırköy-İstanbul) Kuvaterner istifinin sedimanter jeolojisi ve paleoekolojisi, C.Ü. Müh. Fak. Dergisi, 8/1, 93–100

Meriç E, Oktay FY, Sakınç M, Gülen D, Ediger VŞ, Meriç N, Özdoğan M (1991b) Kuşdili (Kadıköy-İstanbul) Kuvaterneri'nin sedimenter jeolojisi ve paleoekolojisi, C.Ü. Müh. Fak. Dergisi, 8/1, 83–91

Okay AI, Sengor AMC, Gorur N (1994) Kinematic history of the opening of the Black Sea and its effect on the surrounding regions. Geology 22:267–270

Okay AI, Kaşlılar-Özcan A, İmren C, Boztepe-Güney A, Demirbağ E, Kuşçu I (2000) Active faults and evolving stike-slip basins in the Marmara Sea, northwest Turkey: a multichannel seismic reflection study. Tectonophysics 321:189–218

Okay AI, Satır M, Tuysuz O, Akyuz S, Chen F (2001) The tectonics of the Strandja Massif: late Variscan and mid-Mesozoic deformation and metamorphism in the north Aegean. Int. J. Earth Sci. 90:217–233

Oktay FY, Gökaşan E, Sakınç M, Yaltırak C, İmren C, Demirbağ E (2002) The effect of North Anatolian Fault Zone to the latest connection between Black Sea and Sea of Marmara. Mar. Geol. 190(1/2):367–382

Orgülü G, Aktar M (2001) Regional moment tensor inversion for strong aftershocks of the August 17, 1999, Izmit Earthquake (Mw = 7.4). Geophys. Res. Lett. 28(2):371–374

Perinçek D (1991) Possible strand of the North Anatolian Fault Zone in the Thrace Basin, Turkey—an interpretation. AAPG Bull 75:241–257

Pınar A, Kuge K, Honkura Y (2003) Moment tensor inversion of recent small to moderate sized earthquakes: implications for seismic hazard on active tectonics beneath the Sea of Marmara. Geophys. J. Int. 153:133–145

Rangin C, Le Pichon X, Demirbağ E, İmren C (2004) Strain localization in the Sea of Marmara: propagation of the North Anatolian Fault in a now inactive pull-apart. Tectonics 23 TC2014. doi:10.1029/2002TC001437

Sakınç M, Yaltırak C, Oktay FY (1999) Paleogeographical evolution of the Thrace Basin and the Tethys–Paratethys relation at northwestern Turkey (Thrace). Palaeogeogr. Palaeoclimatol. Palaeoecol. 153(17):40

Sengör AMC (1979) The North Anatolian Transform Fault; its age offset and tectonic significance. J Geol Soc Lond 136:269–282

Sengör AMC (1980) Türkiye'nin Neotektoniğinin Esasları, TJK. Yayınları

Sengör AMC, Yılmaz Y (1981) Tethyan evolution of Turkey: a plate tectonic approach. Tectonophysics 75:181–241

Sengör AMC, Tüysüz O, İmren C, Sakınç M, Eyidoğan H, Görür N, Le Pichon X, Rangin C (2005) The North Anatolian Fault: a new look. Annu. Rev. Earth Planet. Sci. 33:1–75

Smith AD, Taymaz T, Oktay FY, Yüce H, Alpar B, Başaran H, Jackson JA, Kara S, Şimşek M (1995) High-resolution seismic profiling in the Sea of Marmara (northwest Turkey): late Quaternary sedimentation and sea-level changes. GSA Bull 107(8):923–936

Sunal G, Natal'in B, Satır M, Toraman E (2006) Paleozoic magmatic events in the Strandja Masif, NW Turkey. Geodin. Acta 19:283–300

Tur H (2007) An example of secondary fault activity along the North Anatolian Fault on the NE Marmara Sea Shelf, NW Turkey. Earth Planets Space 59:541–552

Tur H, Icik CE, Aysal N, Koral H (2013) Investigation of the Büyükçekmece and Küçükçekmece Lagoons using Geophysical and Geological Data. The 20th International Geophysical Congress and Exhibition of Turkey, 25–27 November Antalya, Turkey

Yaltırak C (2002) Tectonic evolution of the Marmara Sea and its surroundings. Mar. Geol. 190(1–2):493–529

Yıldırım M, Özaydın K, Erguvanlı A (1992) İstanbul Boğazı güneyi ve Haliç'in jelojik yapısı ve geoteknik özellikleri. Jeoloji Mühendisliği 40:5–14

Yildiz SS, Karaman H (2013) Post-earthquake ignition vulnerability assessment of Küçükçekmece District. Nat. Hazards Earth Syst. Sci. 13:3357–3368

Yılmaz Y and Sakınç M (1990) İstanbul Boğazı'nın Jeolojik Gelişimi Üzerine Düşünceler, İstanbul Boğazı Güneyi ve Haliç'in Geç Kuvaterner (Holosen) Dip Tortulları, Ed: Engin Meriç, İTÜ Vakfı Yayınları, 99–105